Pre-hatch Sexing for Chicken Embryo Based on Immuno-interrogation

Sofhian Ali

Thesis submitted to the University of Ottawa
In partial fulfillment of the requirements for the
Master's degree in Cellular and Molecular Medicine

Department of Cellular and Molecular Medicine
Faculty of Medicine
University of Ottawa

© Sofhian Ali, Ottawa, Canada, 2025

Acknowledgments

I would like to express my deepest gratitude to my supervisor, **Prof. Maxwell Hincke**, for his support throughout my journey. His encouragement and energy pushed me to present my best work. I have learned a great deal from him, not only at the scientific level but also at the personal and professional levels, as a great leader. My sincere appreciation extends to the research associate and Dr. Hincke's lab manager, **Dr. Tamer Ahmed**, whose critical role in keeping everything running smoothly cannot be overstated. His vast experience, constant support, and willingness to share his knowledge have greatly benefited our entire team. Special thanks to my TAC members, Dr. Erik Suuronen and Dr. Qiao Li, for their insightful advice and continuous support of my research. I am also grateful to all the Hincke's lab members for their invaluable help and support. Their camaraderie and assistance have made this journey more enjoyable and fulfilling. Lastly, I am immensely grateful to my parents for their love, prayers and care in helping me reach this milestone. This research was funded by Egg Farmers of Canada, Canadian Poultry Research Council and NSERC. Their support is deeply appreciated.

Abstract

Intensive selection for commercial poultry production has resulted in highly divergent layer and broiler pedigree lines. However, the sex ratio after hatching remains approximately 1:1, resulting in a large-scale culling of male chicks in the industrial egg-laying sector, which raises concerns about animal welfare and ethics. Therefore, early (pre-hatch) sex identification is considered to be essential to address ethical / animal welfare issues, and the Canadian egg production industry aims to discontinue the practice of killing male chicks after hatching. Determining the sex of the chick embryo using non-invasive or minimally invasive approaches before hatching is the focus of intensive research. In birds, males possess the ZZ genotype, and females the ZW genotype; therefore, sex is determined by the presence of the W sex chromosome. The detection of W chromosome–encoded protein(s) in embryonic tissues may allow for sex prediction. We hypothesized that W-encoded proteins may be detectable in the chorioallantoic membrane (CAM), an extraembryonic tissue, using immunochemical approaches. The objective of this research project was to develop and validate an innovative immunochemical approach for sex determination *in-ovo* by detecting the presence of CAM protein(s) encoded on the W chromosome at an early embryonic day (ED 6, 8, or 10). In this study, various CAM manipulation techniques were identified and evaluated, including the use of eggshell (ES) surface disinfectants, ES drilling, various surgical tools and sealant methods. My results indicated that CAM at ED 6 is more challenging to sample, with lower retention of embryo viability (assessed at ED 16) than at ED 8 and 10, which are more compatible with embryo viability. LC/MS/MS-based proteomics was utilized to evaluate the protein profile of CAM tissue harvested at embryonic days (ED) 6, 8, 10, and 12, in order to highlight the expression of distinct CAM functionalities during embryonic development and to gain insight into possible sex-based differences. A total of 2,688 CAM

proteins were identified, with 2,347, 2,265, 2,351, and 1,267 proteins detected at ED 6, 8, 10, and 12, respectively. Notably, 1,191 common proteins were identified across all stages, while 124, 47, 86, and 2 proteins were uniquely expressed at ED 6, 8, 10, and 12, respectively. Notably, a sex-specific analysis identified 614, 320, 314, and 212 proteins that were uniquely expressed in female embryos, and 212, 273, 144, and 56 proteins only in male embryos at ED 6, 8, 10, and 12, respectively. The project's future focus will be to develop and utilize sensitive, specific polyclonal antibodies against synthetic peptides for W-encoded protein(s), with the goal of optimizing an immunoassay for one or more candidate W chromosome-linked proteins in CAM tissue. These findings highlight the potential of CAM in both research and biomedical applications, as well as providing a basis for the development of *in-ovo* sexing technology.

TABLE OF CONTENTS

ABBREVIATIONS

A2M:	Alpha-2-macroglobulin
ACTG1:	Actin, gamma 1
AI:	Artificial Intelligence
ALB:	Albumin
ANXA1:	Annexin A1
ANXA2:	Annexin A2
ANXA5:	Annexin A5
ANXA6:	Annexin A6
ATP1B1:	Sodium/potassium-transporting ATPase subunit beta-1
ATP2A2:	Sarcoplasmic/endoplasmic reticulum calcium ATPase 2
ATP2B4:	Plasma membrane calcium-transporting ATPase 4
ATP6V1E1:	V-type proton ATPase subunit E1
ATP6V1G1:	V-type proton ATPase subunit G1
BCA:	Bicinchoninic acid
CAB39:	Calcium-binding protein 39
CA2:	Carbonic anhydrase II
CA9:	Carbonic anhydrase IX
CA13:	Carbonic anhydrase XIII
CALB1:	Calbindin 1
CALM1:	Calmodulin-1
CALR:	Calreticulin
CAM:	Chorioallantoic membrane
CAMK2D:	Calcium/calmodulin-dependent protein kinase type II delta chain
CDH5:	Cadherin (vascular endothelial)
CDC42:	Cell division control protein 42 homolog
CFIA:	Canadian Food Inspection Agency
CHP1:	Calcineurin B homologous protein 1
COL1A1:	Collagen type I alpha 1 chain
COL1A2:	Collagen type I alpha 2 chain
COL4A1:	Collagen type IV alpha 1 chain
COL4A2:	Collagen type IV alpha 2 chain
COLEC12:	Collectin subfamily member 12
CTSK:	Cathepsin K
DAVID:	Database for Annotation, Visualization, and Integrated Discovery
DCN:	Decorin
DIN:	Drug Identification Number
DSP:	Desmoplakin
ECM:	Extracellular matrix

ED:	Embryonic day
ELISA:	Enzyme-Linked Immunosorbent Assay
emPAI:	Exponentially modified Protein Abundance Index
ES:	Eggshell
ESM:	Eggshell membrane
EU:	European Union
F2:	Thrombin
FBN1:	Fibrillin-1
FCR:	Feed Conversion Ratio
FDR:	False discovery rate
FGA:	Fibrinogen alpha chain
FGB:	Fibrinogen beta chain
FGG:	Fibrinogen gamma chain
FLNA:	Filamin A
FN1:	Fibronectin 1
FTH1:	Ferritin heavy chain 1
FUCA2:	Alpha-L-fucosidase 2
gDNA:	Genomic DNA
GC:	Global control
GO:	Gene Ontology
GSTK1:	Glutathione S-transferase kappa 1
GSTA2:	Glutathione S-transferase alpha 2
GSTA3:	Glutathione S-transferase alpha 3
GSTA4:	Glutathione S-transferase alpha 4
HBA1:	Hemoglobin subunit alpha-1
HBAD:	Hemoglobin subunit delta
HBBA:	Hemoglobin subunit beta-A
HBBR:	Hemoglobin subunit beta-R
HBE/HBE1:	Hemoglobin subunit epsilon-like
HBZ:	Hemoglobin subunit zeta
HNRNPKL:	Heterogeneous nuclear ribonucleoprotein K-like
IC:	Internal control
ILK:	Integrin-linked kinase
JUP:	Junction plakoglobin
KEGG:	Kyoto Encyclopedia of Genes and Genomes
KLH:	Keyhole Limpet Hemocyanin
LC/MS/MS:	Liquid chromatography-tandem mass spectrometry
LYZ:	Lysozyme C
LUM:	Lumican
MAPK3:	Mitogen-activated protein kinase 3

MRC2:	Mannose receptor C type 2
MRI:	Magnetic Resonance Imaging
MMP2:	Matrix metalloproteinase-2
MYH9:	Myosin heavy chain 9
MYL12A:	Myosin light chain 12A
MYOF:	Myoferlin
NEDD4L:	NEDD4-like E3 ubiquitin protein ligase
NCBI:	National Center for Biotechnology Information
NRP1:	Neuropilin-1
PBS:	Phosphate-buffered saline
PCR:	Polymerase Chain Reaction
PDIA4:	Protein disulfide-isomerase A4
PDIA6:	Protein disulfide-isomerase A6
PDLIM3:	PDZ and LIM domain protein 3
POFUT1:	Protein O-fructosyltransferase 1
POFUT2:	Protein O-fructosyltransferase 2
POSTN:	Periostin
PRDX1:	Peroxiredoxin 1
PRDX4:	Peroxiredoxin 4
PRDX6:	Peroxiredoxin 6
PSMA1:	Proteasome subunit alpha type-1
PSMB1:	Proteasome subunit beta type-1
PSMG1:	Proteasome assembly chaperone 1
qPCR:	Quantitative Polymerase Chain Reaction
RH:	Relative humidity
RP:	Reversed-phase
S100A10:	Protein S100-A10
S100A11:	Protein S100-A11
SERPINA10:	Protein Z-dependent protease inhibitor
SERPINB1:	Serpin family B member 1
SERPINB5:	Serpin family B member 5
SERPINB6:	Serpin family B member 6
SERPINH1:	Serpin family H member 1
SLC4A1:	Solute carrier family 4 member 1 (anion exchanger 1)
SOD1:	Superoxide dismutase 1
SOD2:	Superoxide dismutase 2
SPARC:	Secreted protein acidic and rich in cysteine
SPINK5:	Serine peptidase inhibitor Kazal type 5
SPINK7:	Serine peptidase inhibitor Kazal type 7
STIM1:	Stromal interaction molecule 1

SULT1B1:	Sulfotransferase family 1B member 1
SULT1C3:	Sulfotransferase family 1C member 3
SULT1E1:	Sulfotransferase family 1E member 1
SWIM:	SWIM-type zinc finger domain-containing protein
TF:	Serotransferrin
TFRC:	Transferrin receptor protein 1
TLN1:	Talin-1
TNC:	Tenascin C
TXN:	Thioredoxin
VCAM1:	Vascular cell adhesion molecule 1
VCL:	Vinculin
VIM:	Vimentin
VMO1:	Vitelline membrane outer layer protein 1 homolog
VWF:	Von Willebrand factor
WB:	Western Blotting
W:	W chromosome (female-specific sex chromosome in birds)
XHO-I:	XhoI restriction site (genetic marker)
Z:	Z chromosome (sex chromosome in birds)
ZZ:	Male genotype (homozygous Z chromosomes)
ZW:	Female genotype (heterozygous Z and W chromosomes)

LIST OF FIGURES

LIST OF TABLES

Chapter 1: General Introduction

1.1 Overview of the Poultry Industry

The poultry industry is a rapidly growing agricultural sector worldwide, driven by rising demand for meat and eggs. A 2.8% linear growth in poultry production was documented from 2000 to 2020 (Castro et al., 2023), contributing to global food security and economic development. The agricultural sector plays a crucial role in human nutrition by providing high-quality protein from broilers (meat) and layers (table eggs) (Naushad Khan et al., 2021). Due to the increasing global demand for high-quality protein, the poultry industry has taken measures to meet this need, including technological advancements that focus on productivity and sustainability. The poultry industry's intensive selection of pedigree birds for specialized egg and meat commercial production has yielded highly divergent layer and broiler lines. Poultry farming ranges from small-scale farms to industrial-scale factories. Several factors are controlled to optimize table egg and meat production, including feed control, bird housing, lighting, and monitoring flock health, to achieve maximum production of high-quality eggs (laying sector) and broiler meat. For example, one popular layer strain is the White Leghorn chicken, which consistently lays between 250 and 300 eggs per year under standard rearing conditions (Kummer, 2023). Annually, about 1.65 trillion eggs are produced worldwide (Ahmed et al., 2023). In 2024, egg production in Canada reached 915.0 million dozen, representing a 4.3% increase from the 884.0 million dozen produced in 2023, thus a significant contributor to Canada's economy, generating poultry products worth $4.4 billion and accounting for 7.1% of cash receipts in farming operations (Government of Canada, 2025).

1.2 Male Chick Culling: A growing Concern

While poultry operations maintain strict standards and emphasize animal welfare, the practice of culling within the layer sector remains a noted concern. Incubating and maintaining eggs require significant resource investment (time and electricity), thereby creating competitive challenges within the layer industry (Gautron et al., 2021). Chick culling refers to the elimination/euthanasia of 1-day-old male chicks, which are deemed economically nonviable because they do not lay eggs (de Haas et al., 2021), and persists as a critical ethical and economic constraint in intensive layer poultry production. Unfortunately, this practice accounts for the death of approximately 22.5 million male chicks annually in Canada alone (Epp, 2019) and 7 billion worldwide (Krautwald-Junghanns et al., 2018). Some of the standard methods to cull 1-day-old male chicks include asphyxiation using carbon dioxide to render them unconscious, followed by maceration (grinding of chicks in a high-speed grinder) or cervical dislocation (breaking the neck) (Baker et al., 2019). Culling of male chicks raises ethical and animal welfare concerns, and many animal rights movements, scientists and consumers have questioned the need to cull healthy animals based on sex and their intended use (Krautwald-Junghanns et al., 2018). A survey by de Haas et al. (2021) reported that 78% of Dutch citizens disapproved of male chick culling due to concerns about animal rights. In 2020, the European Union (EU) produced approximately 116 billion eggs, equivalent to 7.2 million tons, representing 9.4% of the world's total egg production (Bonnefous et al., 2022). The EU has already implemented policies that ban the practice of culling 1-day-old male chicks (Di Concetto et al., 2023). The industry is seeking alternative solutions and policies for male chick culling and has heavily invested in research to develop them. Moreover, technologies addressing this issue would provide industrial players in the poultry sector with a competitive advantage.

1.3 Industry's Response and the Need for Alternatives

A solution is sought to address ethical, environmental, and economic pressures to avoid culling 1-day-old male chicks (Gautron et al., 2021). The male chicks of the highly selected layer lines are not suitable for meat production due to slower growth and lower feed conversion efficiency compared to broiler lines (Corion et al., 2023). Thus, there are two potential avenues to reduce culling of 1-day-old chicks: developing dual-purpose chicken strains or applying *in-ovo* sexing methods. A dual-purpose chicken strain is a breed in which hens produce eggs for the egg-laying sector, while males of the same breed are used for meat production (Mueller et al., 2018). While this approach would avoid male chick culling, it is not yet economically viable because dual-purpose strains cannot compete effectively with specialized broiler or layer lines. Therefore, this solution is not considered competitive in the global market (Mueller et al., 2018), since selection strategies to optimize weight gain or egg mass produced per unit of feed consumed have not yet been fully explored or optimized for dual-purpose lines (Akinbobola et al., 2021). Overall, it is considered very challenging to raise birds for both high-quality eggs and meat production; thus, the dual-purpose strain is likely to be a very expensive alternative.

Traditional sexing methods have been developed for sexing 1-day-old chicks after hatching (current practice of post-hatch culling); some prominent approaches used in the industry are vent (cloacal) sexing, which is the inspection of morphological sex features, or feather-based sexing based on the examination of offspring chicks that hatch with sex-specific slow or fast growth feathers based on parental crossbreeding (England et al., 2021). An extensively investigated and increasingly prominent strategy to address the male chick culling dilemma is *in-ovo* sex determination. These methodologies encompass techniques that enable embryonic sex identification before hatching, thereby permitting termination during early development. It is

widely considered that avian embryos lack functional nociceptive capacity until embryonic day (ED) 13 (Kollmansperger et al., 2023), and persist in a quiescent, sleep-like neurophysiological state until ED 19. This recognition favours the development of *in-ovo* solutions for sex identification at early embryonic days based on two major underlying themes. Firstly, *in-ovo* sex determination must be minimally or non-invasive, without affecting embryo viability, growth, development, or hatchability. Moreover, this procedure must be rapid, cost-efficient, and accurate (Krautwald-Junghanns et al., 2018). Secondly, embryo sex identification must occur very early in the 21-day incubation period, before hatching, as male embryos must be identified and culled at an early, non-sentient embryonic stage. Some technologies that are almost or already on the market include Hypereye (Göhler et al., 2017), Seleggt (Ching et al., 2023), Agri Advanced Technologies (Ching et al., 2023), Ella *in-ovo* (Oudshoorn, 2023), and Orbem (Hendrix Genetics, 2023). Hypereye, a Canadian company, has developed a non-invasive approach that utilizes hyperspectral imaging and AI to predict the presence of an embryo, its viability, and sex-specific features as early as ED 4 (Göhler et al., 2017). Seleggt, a German-based company, uses technology based on the detection of a sex-specific estrone hormone as early as ED 9, which is associated with the female embryo and can be used to predict whether the embryo is female or male (Ching et al., 2023). Agri Advanced Technologies, another German company, uses hyperspectral technology similar to Hypereye for early sex prediction. IN OVO is a German-based technology company that specializes in *in-ovo* sexing and has developed a technology called Ella. The methodology proceeds by aspirating a minimal volume of fluid from the egg on embryonic day 9 of incubation for subsequent molecular interrogation of sex-specific biomarkers (Oudshoorn, 2023). Orbem, a German biotechnology company, utilizes AI-integrated MRI platforms to achieve non-invasive *in-ovo* sex differentiation on incubation days 11–12 (Hendrix Genetics, 2023). These technological

solutions are under iterative refinement and industrial calibration, with Hypereye and Seleggt demonstrating validated pilot-scale deployment while sustaining progressive optimization trajectories.

1.4 Embryonic Development in Chickens

The domestic chicken (Gallus gallus domesticus) is a rigorously delineated model for developmental biology, angiogenesis, and metastatic cancer research. A principal attribute underpinning the chick embryo's utility in biomedical sciences is its experimental accessibility, coupled with its morphogenetic stages unfolding within a condensed 21-day incubation interval (Nowak-Sliwinska et al., 2014). Avian embryogenesis initiates immediately after fertilization and proceeds through a succession of highly conserved morphodynamic phases, as described by Hamburger and Hamilton (1951; 1992) in their seminal work, which described 46 distinct developmental stages. Figure 1.1 illustrates progressive chick embryogenesis across the 21-day trajectory, concomitant with weight increases in embryonic biomass. The earliest developmental window is particularly pivotal, during which the trilaminar germ layer specification of ectoderm, mesoderm, and endoderm establishes the primordia of all major organ systems (DeRuiter & Doty, 2011). By embryonic days 2-3, cardiogenesis initiates with myocardial contraction, establishing circulatory function (Tong et al., 2013). At the same time, the formation of extraembryonic tissues begins (Lee et al., 2025). From the onset of embryo completion, it exhibits significant growth between embryonic day 3 and 5, including the formation of limb buds (Tong et al., 2013) and attachment of the chorioallantoic membrane (CAM) to the eggshell membrane (Nowak-Sliwinska et al., 2014). Around day 5 to 6, the CAM, a highly vascularized extraembryonic membrane, begins to form through the fusion of the chorion and allantois (Gabrielli & Accili, 2010). As the CAM

develops, the vascular network significantly expands as the embryo grows (Nowak-Sliwinska et al., 2014). This structure becomes functionally mature between days 10 and 12, playing essential roles in gas exchange, calcium absorption from the eggshell, and the management of metabolic waste (Gabrielli & Accili, 2010). Research indicates that chick embryos do not acquire the neurological capacity for nociception (the ability to perceive pain) until approximately ED13, with functional pain perception likely developing closer to ED19 (Kollmansperger et al., 2023). This creates a crucial ethical and biological window before ED13 during which interventions such as sex identification or embryo selection and culling can take place. Early embryogenesis presents multiple potential substrates for biomolecular interrogation, encompassing embryonic fluids, vascular compartments, and extraembryonic matrices such as the CAM. These substrates enable the detection of genomic, proteomic, or metabolomic sex-specific signatures, leading to the claims of emerging commercial platforms (e.g., Seleggt, Hypereye) to evaluate distinct embryonic tissues or molecular biomarkers as promising translational pathways for minimally invasive or non-invasive *in-ovo* sex determination technologies. Consequently, delineating the milestones of embryonic development is indispensable for optimizing alternatives to male chick culling, particularly those that require intervention before the onset of nociception or the establishment of complex neural circuitry.

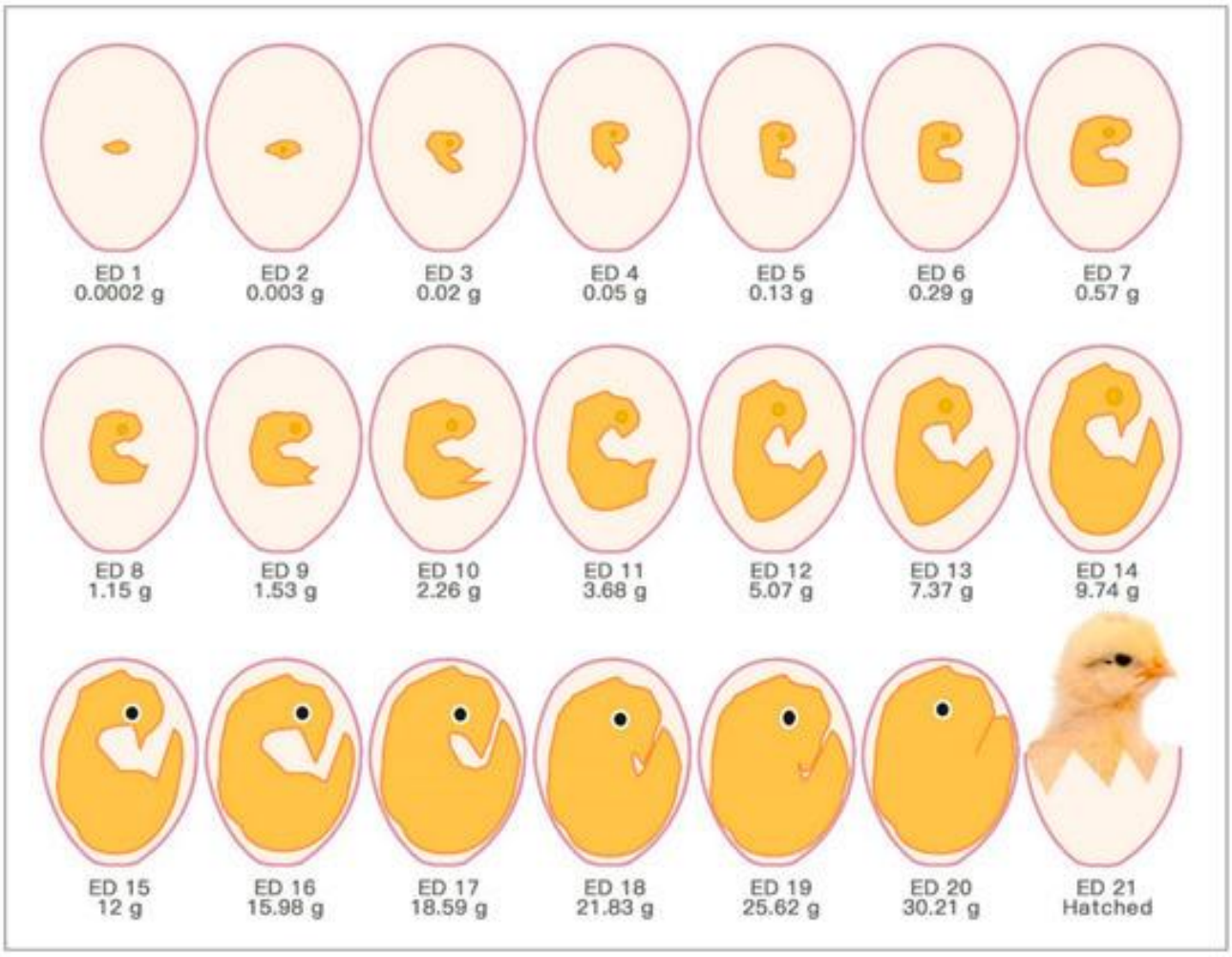

Figure 1.1. Development of the chick embryo through its embryonic life (Chen et al., 2021).

Source: Reproduced from: Chen L., Zhang Y., Li J., et al. Utilisation of Chick Embryo Chorioallantoic Membrane as a Model Platform for Imaging-Navigated Biomedical Research. Cells. 2021;10(2):463. © 2021 by the authors. Distributed under the terms and conditions of the Creative Commons Attribution (CC BY) license (http://creativecommons.org/licenses/by/4.0/).

1.5 Chorioallantoic Membrane (CAM)

The CAM, an extraembryonic membrane, is a highly vascularized and sophisticated structure. The CAM is a vital tissue essential for the embryo's growth and development. There are four extraembryonic membranes: the yolk sac, amnion, chorion and allantois (Raghunath, 2016). The partial fusion of the chorionic and allantoic membranes forms the CAM, as shown in Figure 1.2. The CAM structurally consists of three layers derived from embryonic tissues: the outer chorionic epithelium, a middle layer of vascularized mesoderm, and the inner allantoic epithelium, which lines the allantoic cavity (Gabrielli & Accili, 2010). The CAM forms between days 5 and 6 and surrounds the embryo by days 11 and 12 (Gabrielli & Accili, 2010), during which critical expansion of the vascular system gives rise to the vascular plexus, a rich, concentrated layer of blood vessels (Nowak-Sliwinska et al., 2014). The vast, sophisticated, and rich vessels and structures of the CAM play critical roles in embryonic development. The CAM serves as the embryo's primary respiratory unit due to its vascularized nature, facilitating the exchange of metabolic gases. This permits respiration essential for robust growth and development, as well as supporting its viability. The CAM also facilitates the mobilization of calcium from the calcareous shell into the embryonic compartment and intracellular transport, as well as systemic acid–base equilibrium, and reabsorption of water and electrolytes, while modulating excretory urination; these physiological functions are partitioned between the chorionic and allantoic epithelia (Gabrielli & Accili, 2010). The CAM is also an important tissue in biomedical applications for various studies, such as angiogenesis, due to its vascularized network of blood vessels, which is suitable for *in vivo* studies (Nowak-Sliwinska et al., 2014).

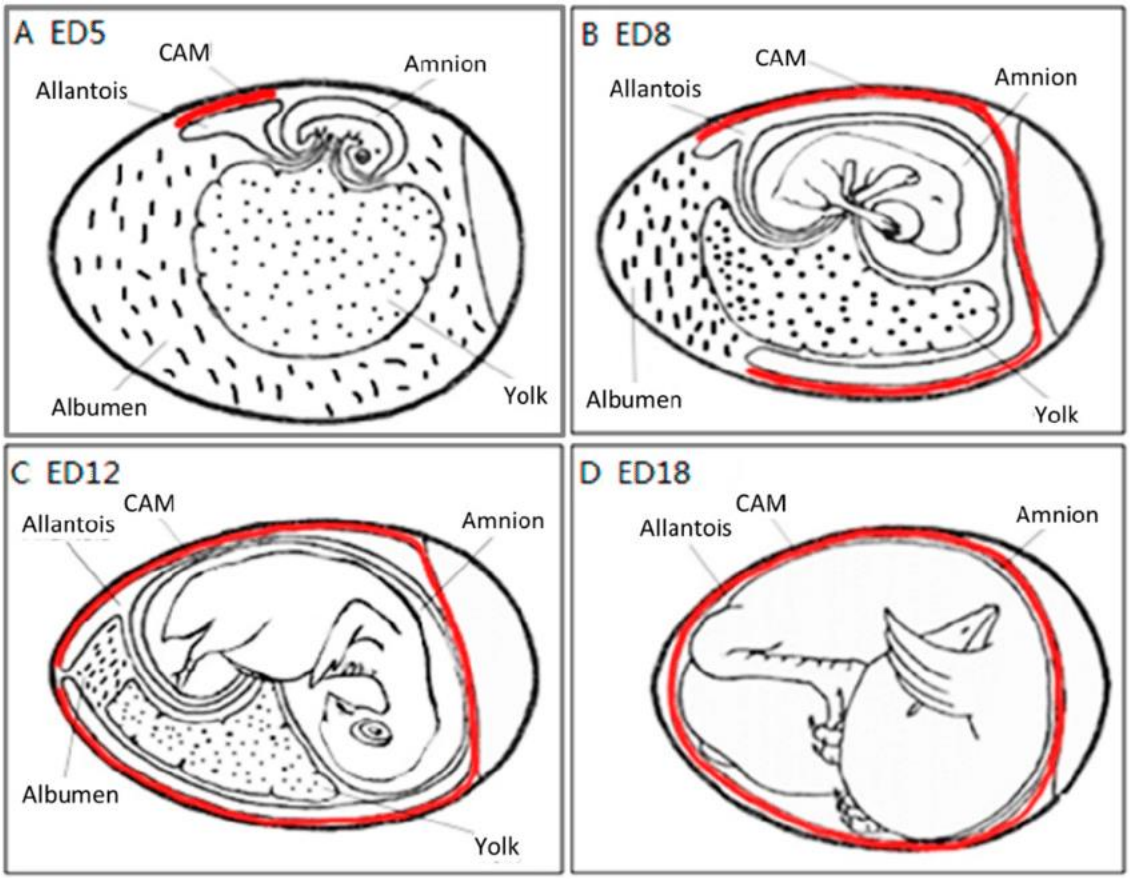

Figure 1.2. Development of the CAM during embryonic life (Chen et al., 2021).

Source: Reproduced from: Chen L., Zhang Y., Li J., et al. Utilisation of Chick Embryo Chorioallantoic Membrane as a Model Platform for Imaging-Navigated Biomedical Research. Cells. 2021;10(2):463. © 2021 by the authors. Distributed under the terms and conditions of the Creative Commons Attribution (CC BY) license (http://creativecommons.org/licenses/by/4.0/).

1.6 Sex Determination in Chickens

In avian species, sex is determined by the Z and W sex chromosomes; however, the configuration of these chromosomes is the opposite of that in mammalian species. For example, humans have XY heterozygous chromosomes in males, and XX homozygous chromosomes in females. In avian species, males are ZZ homozygous, and females are ZW heterozygous (Bellot et al., 2017). The Z

chromosome is larger and more gene-rich, containing over 1,000 genes. In contrast, the W chromosome, which is significantly smaller than the Z chromosome, contains only 28 coding genes (Lin et al., 2023). Sex determination in avian embryos can be resolved by interrogating sex-linked loci, such as SWIM and XHO-I, which are located on the female-specific W chromosome. Molecular assays that ascertain the presence or absence of W chromosome-restricted genes permit accurate prediction of embryonic sex. Discrimination between male and female embryos is routinely achieved via polymerase chain reaction (PCR) amplification (Gautron et al., 2021), in which W-specific genetic markers are contrasted with a housekeeping gene (e.g., 12S rRNA) expressed in both sexes. Thus, the identification of embryonic sex by detecting W-chromosome–encoded proteins on the chorioallantoic membrane is a potential diagnostic approach. In our preliminary proteomic experiments, four CAM proteins were detected, encoded on the W chromosome, and may serve as potential markers for predicting the female embryo. In subsequent trials, we identified three additional candidates as potential biomarkers. These results served as the basis for the research motivation of this project to develop a novel alternative approach to identify female chick embryos at an early developmental stage, thereby reducing reliance on the current practice of culling 1-day-old male chicks. This project seeks to develop an accurate and rapid pre-hatch sexing technique for the immunochemical identification of one or more W-encoded proteins in CAM at an early embryonic age (ED6-10). Our study focused on using the readily accessible extraembryonic CAM membrane to develop a novel method for sex determination. We explored methods to manipulate/sample the CAM without compromising embryo viability, in order to interrogate a CAM protein biomarker encoded on the W chromosome (specific to female embryos), for embryo sex identification.

1.7 Project Overview

This project aims to develop a non-lethal, early-stage method for sex determination in chick embryos using the CAM as a platform, based on two key hypotheses: 1) embryonic viability will be unaffected or minimally impacted by sampling a minute quantity of CAM suitable for immunological interrogation; 2) a pre-hatch sexing technique can be developed based on the immunochemical identification of W-encoded protein(s) in CAM at an early embryonic age. Therefore, the overall project objectives include:

1. Optimize the CAM tissue sampling procedure, location, and amount at the earliest embryonic stage, with preservation of embryo viability.
2. Identify W-encoded proteins in the CAM of female embryos at early embryonic development, utilizing proteomics and bioinformatics.
3. Generate polyclonal antibodies against synthetic peptides that represent epitopes of candidate W-linked proteins.
4. Develop and refine an immunoassay, such as ELISA, for rapid, sensitive, and precise detection of W-encoded proteins.

This project seeks to provide a practical alternative to post-hatch chick culling, offering a scalable approach to early sex prediction in the poultry industry. The thesis describes the work to address the first two objectives, with objectives 3 and 4 being briefly touched upon, as further optimization of these objectives is still ongoing.

Chapter 2: Hypothesis and Objectives

2.1 Hypotheses

1. Embryonic viability, growth, and development will be unaffected or minimally affected by sampling a minute quantity of chorioallantoic membrane (CAM) suitable for immunological interrogation.
2. An accurate and rapid pre-hatch sexing technique can be developed based on the immunochemical identification of W-encoded protein(s) in CAM at an early embryonic age (ED6-10).

2.2 Objectives

1. Optimize the CAM tissue sampling procedure, location, and amount at the earliest embryonic stage for immunochemical-based detection of specific W-encoded protein(s).
2. **2a.** Identify W-encoded proteins in the CAM at early embryonic development utilizing proteomics and bioinformatics.

   2b. Use qPCR for a W-specific gene to validate the proteomics-based sex prediction.

PREAMBLE TO CHAPTERS 3 AND 4

Chapters 3 and 4 present the experimental and analytical chapters of this thesis, which have each been submitted for publication in the peer-reviewed literature. Chapter 3 examines the effect of early-stage CAM manipulation and sampling at embryonic days (ED) 6, 8, and 10 on embryo viability at ED 16, in relation to objective 1 of the project. This chapter examines the impact of various procedural variables, including eggshell disinfection methods, eggshell drilling, membrane removal, CAM sampling techniques, and sealing strategies, on survival outcomes. These results establish practical boundaries for the safe and effective interrogation of the CAM, forming a critical foundation for the development of early-stage, non-lethal sexing methodologies. Chapter 4 builds upon this foundation by applying LC/MS/MS-based proteomic analysis to CAM tissue collected at ED6, 8, 10, and 12. This analysis profiles the CAM proteome across developmental stages, identifying protein constituents and describing their functional roles. Importantly, the study identifies CAM proteins linked to embryo sex. By connecting developmental proteomic changes to sex-specific molecular signatures, Chapter 4 demonstrates the CAM's potential as both a biological target with an array of functional and molecular distinctions and as a diagnostic platform for sexing technologies. Together, these chapters integrate procedural feasibility with molecular discovery, directly advancing the thesis objective of establishing the CAM as a viable, ethical, and scientifically robust platform for early, non-invasive sex determination in poultry.

Chapter 3: Effect of early chorioallantoic membrane manipulation on chicken embryo viability

Short Communication: Effect of early chorioallantoic membrane manipulation on chicken embryo viability

Sofhian Ali[a], Tamer A. E. Ahmed[a] and Maxwell T. Hincke[a,b] *

[a]Department of Cellular and Molecular Medicine, Faculty of Medicine, University of Ottawa, Ontario, K1H 8M5, Canada.

[b]Department of Innovation in Medical Education, Faculty of Medicine, University of Ottawa, Ontario, K1H 8M5, Canada.

Author's name:

Sofhian Ali

Tamer A. E. Ahmed

Maxwell T. Hincke

Corresponding authors:

Maxwell T. Hincke

This chapter corresponds to a manuscript submitted for peer-reviewed publication to the Journal of Veterinary and Animal Sciences.

ABSTRACT

The chorioallantoic membrane **(CAM),** a vascularized extraembryonic membrane of the developing chick embryo, is widely utilized in biomedical research. There is a growing interest in pre-hatch embryo sex determination to eliminate the current practice of culling 1-day-old male chicks in the layer industry, and CAM interrogation may provide this information. The objective of the current study was to assess the effect of early CAM manipulation on pre-hatching embryo viability at embryonic day 16 **(ED16),** since reliable access to CAM without compromising embryo survival is essential for a strategy of sex determination during early embryogenesis. Early sexing techniques based on CAM-derived biomarkers could offer an ethically acceptable alternative to post-hatch sexing determination. This study assessed the effects of early CAM manipulation (ED6, 8, and 10) in chicken embryos, focusing on comparisons of egg disinfection, eggshell (ES) drilling, eggshell membrane (ESM) puncture, CAM sampling, and ES sealing strategies. Our results showed that manipulating CAM at ED6 was associated with reduced viability compared with ED8 and ED10 under various conditions. CAM manipulation at ED6 results in 0% viability, while viability was partially retained at ED8 (44%) or ED10 (42%). CAM sampling was associated with elevated mortality on ED6 (0% viability), ED8 (11%) and ED10 (30%). Our research demonstrates that early manipulation or sampling of CAM has a deleterious impact on embryo viability, especially at the earliest time points. Therefore, data collected on the manipulation of the CAM have helped establish a foundation for developing early-stage sex-determination methods.

Keywords: Chorioallantoic membrane; Developmental manipulation; Embryonic viability; Layer chicken; *In-ovo* sexing

1. INTRODUCTION

The avian embryo is a valuable in vivo model for studying angiogenesis, cancer, and biomedical research due to its accessibility and rapid development (Nowak-Sliwinska et al., 2014). The chorioallantoic membrane (CAM) is a multifunctional and essential organ for chicken embryo development (Gabrielli & Accili, 2010). The CAM is the primary respiratory organ of the embryo, and regulates acid-base homeostasis; moreover, it mediates calcium transport from the eggshell (ES) to the developing embryo (Gabrielli & Accili, 2010). Many studies on angiogenesis and metastasis have used the CAM as an experimental model, as its blood vessel pattern is highly visible, allowing observation of tumour progression (Chu et al., 2021). Validating new experimental techniques to assess CAM sensitivity relative to normal embryo development, given its delicate nature, is a crucial step toward maximizing CAM utilization across various biomedical applications. The poultry layer industry is increasingly interested in non-invasive, early-stage sex determination to avoid the controversial practice of culling 1-day-old male chicks, which has drawn growing ethical and negative societal concerns (Gautron et al., 2021). As an accessible extraembryonic tissue, the CAM offers potential for pre-hatch molecular sexing approaches at early developmental stages, if tissue sampling is compatible with embryo viability. Our central hypothesis is that CAM can be safely accessed and sampled at early developmental stages without compromising embryo health or viability. The objective of this study was to assess the effect of various early CAM manipulations at embryonic days (ED) 6, 8, and 10 on viability at ED16. We assessed ES disinfection, drilling, and sealing techniques along with eggshell membrane (ESM) puncture and CAM removal/sampling approaches and identified critical constraints. This information is crucial for developing innovative strategies to utilize

CAM tissue at ED6, 8, and 10 for molecular, immunological, or proteomic assessment without compromising embryo viability.

2. MATERIALS AND METHODS

Fertilized white leghorn eggs were obtained from the Canadian Food Inspection Agency, Ottawa. Eggs were incubated at ED0 in a Petersime Model 1 incubator (Petersime Incubator Co., Gettysburg, Ohio). No ethical approval was required for the *in-ovo* assessments, as all experimental groups and controls were terminated at ED16 by euthanization of embryos (Süß et al., 2023). Eggs were candled (Titan Incubators, Malmesbury, England) to detect and eliminate any cracked or unfertilized eggs. ES drilling to gain access to the interior was performed with a rotary Dremel tool (Jobmate, Canada), equipped with a spherical grinding accessory (0.8, 1.6, 2.4 or 5-mm bit sizes). Insulin syringes (U-100) with 23G or 31G needles were used for the puncture of ESM (Carepoint VET, Allison Medical Inc., Littleton, Colorado). Suction pens (model no. FFQ939 and V-8918ESD) were from a commercial manufacturer (Robe parts and Deeoee, China). Micropipettes (P-200 and P-1000) were from Gilson (Madison, Wisconsin), and the tips were purchased from Ultident (St. Laurent, QC). The disinfectants utilized were Dettol 0.6% (Chloroxylenol, DIN# 003733435), benzalkonium chloride 0.13% (On-the-go antiseptic spray, DIN#02369575) and ethanol 70% (Commercial Alcohols Inc., ON, LOT# 037470). The sealants used were paraffin (LOT# 2403015) was from Leica (Biosystems Richmond, Inc., IL, USA), and Stuck^{TM} thick-gel super glue (cyanoacrylate), silicone glue stick, and mini glue gun were from local suppliers.

2.1 Egg incubation and candling

Eggs were incubated with the broad end facing upwards and automatically rotated every 2 hours (37.0°C; RH 50-60%). Egg weights were recorded at ED0, 6, 8, 10 and 16 (Denver instruments, S403 balance). Embryo weight and sample size (n) for each treatment are listed in Table 3.1. At ED6, when CAM vasculature became visible, unfertilized eggs were identified and eliminated. At ED16, embryo viability was assessed by cracking open the egg, followed by euthanizing via decapitation with surgical scissors. Embryos were then rinsed with deionized water, dried (Kimwipe) and weighed.

2.2 Eggshell surface disinfection

ES surface disinfection was performed using various methods before ES drilling (Jobmate Dremel style spherical-shaped bit to create a 3 mm hole) at ED6, including ethanol (immersion for 20 min or via Kimwipe at a pre-selected sampling site) versus Dettol (chloroxylenol, 0.6%, 5 min), or benzalkonium chloride (0.13%, 10 min), both applied using Kimwipe, with untreated eggs served as a negative control.

2.3 Sampling site

Two sites for CAM sampling were compared: the equatorial region and the broad end near the air sac. The selected sites on the ES surface were marked with a pencil, and a 3 mm hole was drilled at ED 6, 8, or 10, followed by removal of the underlying ESM. CAM was manipulated with fine-point forceps to grip it, and a sample was excised with scissors. The hole in the ES was sealed with silicone via a silicone gun, and incubation was continued until ED16.

2.4 ESM (eggshell membrane) manipulation

After eggshell drilling, the underlying ESM must be punctured to reach the CAM. The effects of ESM manipulation at ED6 on embryo weight and viability were assessed at ED16. Following disinfection with each agent (70% ethanol and Dettol 0.6%), and after selecting a sampling site, the ES was drilled to create a 3 mm hole. The exposed ESM was manipulated using two approaches: a single puncture with a 23G needle or multiple punctures along the edge of the ES hole, followed by removal of the ESM flap with fine-point forceps. These manipulations were then compared to non-manipulated, intact ESM. Finally, the hole in ES was sealed, and incubation was continued until ED16.

2.5 CAM sampling

A hole (3 mm) was created in the disinfected ES surface (Dettol) using a Dremel bit. The ESM was removed as per Section 2.4 to expose the CAM, which was manipulated using three approaches: ESM removal alone; ESM removal and CAM tugging with tweezers without sampling, or ESM removal and CAM sampling using fine-point forceps and scissors to collect a minute fragment (~5 mg). Eggs were sealed and returned to the incubator until ED16, where the embryo weights and viabilities were assessed.

In another series of experiments, 3 different methods of CAM harvesting were compared: The first approach involved the surgical removal of the CAM sample (<5 mg) using fine-point forceps and scissors (as described above). The second approach involved latching onto the exposed CAM with a suction pen before excising the CAM tissue with scissors. The third approach involved using a sterile yellow micropipette tip to suction-latch onto the exposed CAM (200 μL setting) and elevate

it for excision using scissors. Eggs were sealed with silicone and incubated until ED16, where the embryo weight and viability were recorded.

2.6 Sealants

Different sealing strategies were assessed after drilling a hole in the ES surface. Eggs were disinfected with 70% ethanol (Kimwipe application) at ED6, and a 3 mm hole was created using a Dremel. Eggs were then subdivided into two treatment groups: ESM was either left unmanipulated (control) or completely removed by puncturing multiple holes along the ESM edge using a 23-gauge needle, followed by the removal of the flap with forceps. Eggs were then sealed and returned to the incubator until ED16. The following sealants were assessed: cyanoacrylate (crazy glue, full solidification required up to 24 hours); silicone (applied using a silicone gun (130°C), which solidified immediately); and paraffin (melted at ~100.0°C and was applied using a Pasteur pipette and solidified immediately).

2.7 Statistical tests

Statistical analysis was done using IBM SPSS statistical software version 30. A two-tailed *t*-test and ANOVA (one-way with Bonferroni as a post-hoc test) were used for statistical comparisons. All experimental data were expressed as the mean ± SD, with ***$p < 0.001$, **$p < 0.01$, and *$p < 0.05$ considered statistically significant between test groups and the control. (*) indicates a statistically significant difference using ANOVA, with ns: not significant. Results were compared with trial-specific and total controls, designated as internal control (IC) and global control (GC), respectively. Graphs were generated using GraphPad Prism version 10.

3. RESULTS AND DISCUSSION

3.1 Effect of ES surface disinfection upon viability

A commonly used disinfectant is 70% ethanol, which was compared to Dettol and benzalkonium chloride. Our results showed that disinfection with Dettol or benzalkonium chloride showed better embryo viability compared to ethanol. Results indicated that eggs wiped with ethanol exhibited a higher average embryo weight and viability % on ED16 (11.4 ± 2.0 g, 75%) compared to the eggs submerged in ethanol for 20 mins; only one embryo survived (6.3 g, 25%) (Table 3.1). However, wiping with ethanol resulted in a tendency for lower average weight and viability compared to the global control **(GC)** (13.1 ± 1.0 g, 98%), although this difference was not statistically significant. A previous study conducted decontamination of the egg surface with 70% ethanol at ED3, followed by various treatments. Their control results (70% ethanol surface only) indicate embryo survival <90% (Ali Laghari, 2015), consistent with our results. Another study tested the effect of ethanol 70% application on embryo viability from ED1 to ED18, compared to those treated with distilled water immediately post-lay, which demonstrated that ethanol reduced viability, especially within the first five days, to approximately 30% compared to 70% in the sterile water-treated group (Kunz et al., 2019). Herein, different disinfectants tested at ED6, such as ethanol (70%), Dettol (0.6%), and benzalkonium chloride (0.13%), with a 3 mm hole drilling on the ES surface, were compared to control embryo viability at ED16. Dettol-treated eggs (ED16 embryo weight: 15.4 ± 0.9 g) and the benzalkonium chloride group (14.3 ± 1.1 g) were not significantly different from the internal control group (**IC**, 14.8 ± 1.0g) (Table 3.1). In addition, benzalkonium chloride-treated eggs showed embryo weights that were not significantly different from those of GC; however, Dettol-treated eggs exhibited a significantly higher embryo weight compared to GC ($P < 0.05$). Studies about the assessment of different disinfecting agents for CAM manipulation are scarce.

Our findings demonstrated that ED16 embryos from Dettol- and benzalkonium chloride-treated eggs had higher average weights across all groups examined and higher viability than the ethanol-treated group (Table 3.1). Acsa et al. (2021) tested Dettol and Kupacide against different bacterial isolates (*E. coli*, *Staphylococcus* sp. and *Streptococcus sp.*). Kupacide contains benzalkonium chloride (10% v/v). In our treatments, we used 0.13%. They reported that Kupacide and Dettol killed bacterial isolates in a dose-dependent manner (Acsa et al., 2021).

3.2 Effect of CAM sampling location on viability

In our study, the impact of sampling location was assessed by harvesting CAM from the equatorial and broad regions to compare their suitability for CAM sampling without compromising the embryo viability on ED6, 8 and 10. The average ED16 weight of embryos manipulated on ED6 at the equatorial region was 10.4 ± 2.9 g, which was significantly lower (*$P<0.05$) than the IC (14.3 ± 0.8 g) (Table 3.1 and Figure 3.1(D)). In contrast, the average embryo weight when CAM was manipulated at the broad region on ED6 resulted in 100% fatality. CAM is quite delicate and thin around ED5 and 6 as it begins to form; therefore, its manipulation at this early developmental stage is highly disruptive and results in very low viability (Gabrielli & Accili, 2010). At ED8, CAM sampling in the equatorial region yielded 29% viability, with an average embryo weight of 12.3 ± 3.2 g, whereas manipulation in the broad region yielded 11% viability and an embryo weight of 12.5 g (only one surviving embryo). (Table 3.1). Furthermore, manipulation of CAM at the broad region on ED10 resulted in 30% embryo viability and an average embryo weight of 11.9 +/- 1.9 g, while similar manipulation at the equatorial region resulted in 100% fatality (Figure 3.1(D) and Table 3.1). In general, manipulation of CAM at ED8 and ED10 resulted in comparable embryo

weight (not significantly different) from the GC and IC control groups, while the viability was inferior to that of the IC (14.3 ± 0.8 g, 100% viability) (Table 3.1 and Figure 3.1(D)).

3.3 Effect of CAM sampling location on viability

In addition to its crucial role in initiating biomineralization and ES assembly during eggshell formation, the ESM also maintains embryo viability during development, serving as both a physical and chemical barrier against pathogen invasion (Ahmed et al., 2017). In this study, average embryo weight at ED16 after Dettol- disinfection with ESM removal (15.3 ± 1.6 g, $P<0.05$, 80% viability) or with ESM retention (15.3 ± 0.5, $^{**}P<0.01$, 100% viability) were significantly higher than the GC (13.1 ± 1.0 g, 98%) but not significantly different from the IC (figure 3.1(A)). In addition, the average embryo weight at ED16 after disinfection with Dettol and ESM puncture (16.1 ± 0.8 g, $^{***}P<0.001$, 100%) was significantly higher than the GC and was not significantly different from IC (Figure 3.1(A) and Table 3.1). In contrast, eggs disinfected with ethanol before ESM removal (10.8 ± 2.4 g, 75% viability), single puncture of ESM (12.7 g, 25% viability), or disinfected with ethanol without any ESM manipulation showed no significant difference (13.2 ± 1.0 g, 100% viability) compared to GC (13.1 ± 1.0 g, 98%) (figure 3.1(B) and table 3.1).

3.4 Effect of CAM sampling on embryo viability

Herein, the effects of CAM sampling on embryo viability were assessed. The results indicated that when ESM was solely removed at ED6, 8, and 10, the average weight of the embryo at ED16 compared to IC control (13.6 + 0.8g) was 12.0 ± 3.1 g (55%), 13.5 ± 0.7 g (80%) or 14.0 ± 0.9 g (90%) (Table 3.1). As the CAM tissue is well developed at later time points (ED8 and 10), it is more robust and able to tolerate interventions. Our results demonstrated that ESM removal

negatively affected embryo viability (Table 3.1). Mortality was also observed when CAM was pulled or sampled (5mg) at ED6, 8, and 10 (Figure 3.1E, 3.1F). CAM pulling or sampling at ED6 resulted in 100% mortality, whereas embryo viability was improved at ED8 (44%) and ED10 (42%) (Figure 1E). Similarly, CAM sampling resulted in enhanced embryo viability at ED8 (11%) and ED10 (30%), compared to ED6 (Figure 1F). Moreover, either CAM pulling or sampling at ED8 and 10 resulted in better average embryo weights (>10 g) (Figures 3.1E, 3.1F and Table 3.1), compared to ED6.

Surgical removal of CAM (5 mg) is very invasive and requires precise manipulation. Various strategies were employed to minimize the impact on embryo viability, including the use of surgical tools (tweezers and scissors), a suction pen, or micropipette tips that enabled CAM latching via suction rather than physical grasping with tweezers. Three strategies were assessed on ED6, 8 and 10 to assess their impact on embryo viability. The suction generated by the micropipette approach was controllable, with settings ranging from 100 to 200 μL for sampling CAM tissue. The use of disposable, sterile, autoclavable tips minimized the risk of contamination, and the tunable suction minimized the risk of blood vessel rupture. The micropipette group exhibited an embryo weight of 11.5 g and 13% viability at ED6 with one surviving embryo a standard deviation could not be calculated, which was then improved at ED 8 (13.8 ± 1.9 g and 25% viability) and ED10 (13.1 ± 0.4 g and 57% viability), which were not different from the GC and IC values (Figure 3.1I and Table 3.1). Surgical tools (Figure 3.1G) and suction pen-mediated (Figure 3.1H) sampling of CAM at ED6 and 10 resulted in 0% viability at ED16. A notable disadvantage was that the soldering suction pen's negative pressure was not controllable and had a suction equivalent to a micropipette

setting of 800 µL. Therefore, it latched onto a large amount of CAM and also drew up the surrounding albumen.

3.5 Effect of hole closure sealants on embryo development and viability

When a hole in the ES is drilled to access the CAM during various studies, sealing is subsequently required to maintain the microenvironment, water balance, and gaseous exchange, and to prevent pathogen invasion, thereby protecting the developing embryo. Therefore, we tested various sealing strategies and assessed their impact on embryo viability. Yang et al. (2024) assessed parafilm sealing for windowed eggs and reported a negative result in terms of the hatching performance. In the current study, cyanoacrylate glue, paraffin and silicone glue were evaluated. We observed that applying a sealant to an egg with its ESM removed hindered embryo viability and was associated with lower ED16 embryo weight compared to embryos without ESM removal. The utilization of silicone as a sealing strategy in combination with uncompromised ESM (13.2 ± 1.0 g, 100%) or ESM removal (10.8 ± 2.4 g, 75%) showed no significant difference in the embryo weight compared to the GC (13.1 ± 1.0 g, 98%) (Table 3.1 and Figure 3.1(C)). Regarding paraffin sealing, the average embryo weight at ED16, with or without ESM, was 12.9 ± 0.6 g (50% viability) and 10.2 g (25% viability), respectively, and did not differ significantly from the GC. Finally, cyanoacrylate glue needed a much longer time to solidify compared to the other two sealants and was associated with 100% fatality when combined with ESM removal. In contrast, when combined with intact ESM, cyanoacrylate-mediated sealing showed comparable viability (100% viability), and embryo weight (12.8 ± 0.9 g) was not significantly different from that of GC. Based on these findings, silicone was selected as the sealing strategy and used during most experimental manipulations (Figure 3.1(C) and Table 3.1).

4. CONCLUSION

This study demonstrated that early manipulation of the chorioallantoic membrane (CAM) significantly affects chick embryo viability, with the greatest mortality observed at ED6 and improved survival at ED8 and 10. Although viability at ED6 was generally lower across interventions, these data provide a critical foundation for refining sexing protocols that utilize the CAM for early-stage biomolecular analysis, such as protein-based sex markers. This study provides further insight into the challenge of developing innovative strategies to retrieve CAM tissue while retaining embryo viability. The increasing demand for ethical alternatives to male chick culling has driven the need for reliable and non-lethal methods of early sex determination in the poultry layer industry. Among the evaluated conditions, Dettol and benzalkonium chloride proved effective disinfectants, while silicone was the most compatible sealing material. CAM sampling using a micropipette at ED8–10 was associated with higher viability compared to earlier or more invasive methods, suggesting these stages are more suitable for minimally invasive tissue access. Overall, these findings establish key parameters for optimizing CAM manipulation protocols and provide a foundation for developing early, ethical, and biologically viable pre-hatch sex determination techniques.

5. ACKNOWLEDGEMENTS

Funding and support for this study were provided by the Natural Sciences and Engineering Research Council (NSERC-Discovery; NSERC-Alliance), Egg Farmers of Canada (EFC), Canadian Poultry Research Council (CPRC) and Canadian Poultry and Egg Processors Council (CPEPC).

6. Declaration of AI and AI-assisted technologies in the writing process

During the preparation of this work, the authors utilized ChatGPT to enhance the language and readability of a specific component of the discussion. After using this tool/service, the authors reviewed and extensively edited the content as needed, taking full responsibility for the content of the publication.

CRediT: authorship contribution statement:

Sofhian Ali: Investigation, Methodology, Resources, Validation, Formal Analysis, Data Curation, Writing – _original draft, Writing – _review and editing. ***Tamer Ahmed:*** Project administration, Conceptualization, Methodology, Validation, Resources, Writing – _review and editing, Funding acquisition. ***Maxwell Hincke:*** Supervision, Conceptualization, Methodology, Validation, Writing – _review and editing, Funding acquisition.

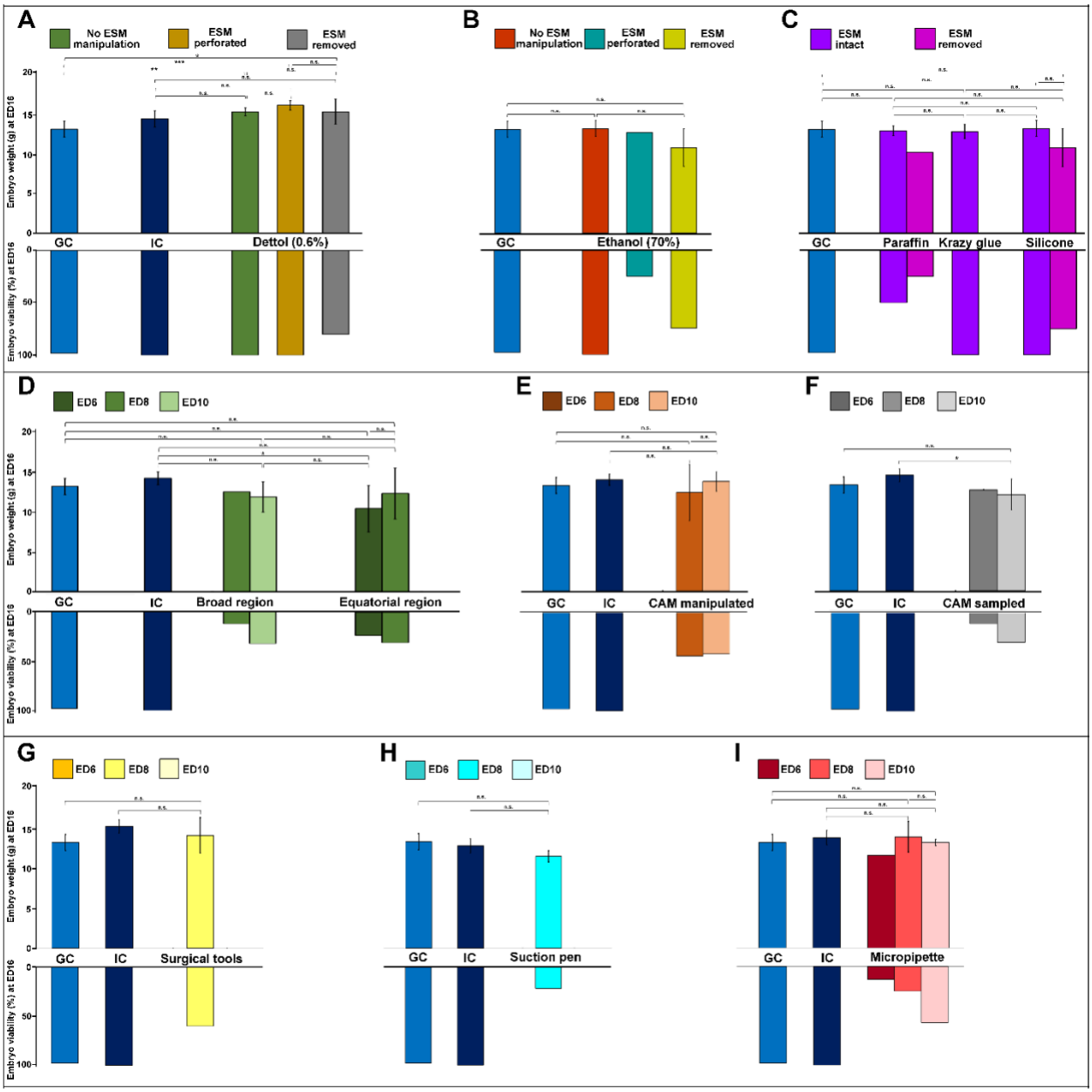

Figure 3.1. Effect of treatments on early development of embryonic viability at ED16. Effect of various early manipulation strategies at ED6 on embryo weight and viability (%), as assessed on ED16 following ES surface disinfection. Dettol 0.6% (A) or ethanol (70%) (B) and sealing (C). Investigated at ED6, 8 and 10 of different CAM manipulation sites (D) and strategies (E-I) as compared to the internal (IC) and global controls (GC). **p < 0.001, **p < 0.01, and *p < 0.05 were statistically significant when comparing different manipulation strategies and controls. NS,

nonsignificant. ESM: Eggshell membrane; CAM: Chorioallantoic membrane; EtOH: Ethanol; BC: benzalkonium chloride; S: Silicone; C: Cyanoacrylate/Super glue; P: Paraffin; mm: millimetre; ED: embryonic day; Y: Yes; N: No; G: Gauge; and -: not tested; n: Sample size

Table 3.1 Summary of manipulations and results for different experimental assessments of embryo weight (g) and viability (%) at ED16.

Assessed manipulation strategy (condition)		Applied manipulation strategy					Embryo weight (g) & Viability (%) at ED16 (n)				
		Disinfection (type)	Drilling (3mm hole)	ESM	CAM	Sealing (type)	ED6	ED8	ED10	Internal CTRL (IC)	Global CTRL (GC)
I. Disinfection	Wiping (EtOH 70 %)	Y (EtOH)	N	N	N	N	11.4 ± 2.0 & 75 (4)	-	-	-	13.1 ± 1.0 & 98 (173)
	Submerging (EtOH 70 %)	Y (EtOH)	N	N	N	N	6.3 & 25 (4)	-	-		
	Wiping (EtOH 70 %)	Y (EtOH)	Y	N	N	N	13.9 ± 0.7 & 75 (4)	-	-	-	
	Wiping (Dettol®, 0.6%)	Y (Dettol®)	Y	N	N	N	15.4 ± 0.9 & 83 (6)	-	-	14.8 ± 1.0 & 100 (5)	
	Wiping (BC, 0.13%)	Y (BC)	Y	N	N	N	14.3 ± 1.1 & 100 (5)	-	-		
II. ESM manipulation	ESM (Intact)	Y (EtOH)	Y	N	N	Y (S)	13.2 ± 1.0 & 100 (4)	-	-	-	
	ESM (Poked once)	Y (EtOH)	Y	Y (23G)	N	Y (S)	12.7 & 25 (4)	-	-		
	ESM (Removed)	Y (EtOH)	Y	Y (23G)	N	Y (S)	10.8 ± 2.4 & 75 (4)	-	-		
	ESM (Intact)	Y(Dettol®)	Y	N	N	Y (S)	15.3 ± 0.5 & 100 (6)	-	-	14.4 ± 1.0 g & 100 (5)	
	ESM (Poked once)	Y(Dettol®)	Y	Y (23G)	N	Y (S)	16.1 ± 0.6 & 100 (6)	-	-		
	ESM (Removed)	Y(Dettol®)	Y	Y (23G)	N	Y (S)	15.3 ± 1.6 & 80 (5)	-	-		
III. Sampling site	Broad region	Y(Dettol®)	Y	Y (23G)	Y	Y (S)	0.0 ± 0.0 & 0 (8)	12.5, 11 (9)	11.9 ± 1.9 & 30 (10)	14.3 ± 0.8 & 100 (8)	
	Equatorial region	Y(Dettol®)	Y	Y (23G)	Y	Y (S)	10.4 ± 2.9 & 22 (9)	12.3 ± 3.2, 29 (7)	0.0 ± 0.0 & 0 (7)		
V. Sealant	Paraffin (Intact ESM)	Y (EtOH)	Y	N	N	Y (P)	12.9 ± 0.6 & 50 (4)	-	-	-	
	Paraffin (Removed ESM)	Y (EtOH)	Y	Y (23G)	N	Y (P)	10.2 & 25 (4)	-	-		
	Cyanoacrylate (Intact ESM)	Y (EtOH)	Y	N	N	Y (C)	12.8 ± 0.9 & 100 (4)	-	-		
	Cyanoacrylate (Removed ESM)	Y (EtOH)	Y	Y (23G)	N	Y (C)	0.0 ± 0.0 & 0 (4)	-	-		
	Silicone (Intact ESM)	Y (EtOH)	Y	N	N	Y (S)	13.2 ± 1.0 & 100 (4)	-	-		
	Silicone (Removed ESM)	Y (EtOH)	Y	Y (23G)	N	Y (S)	10.8 ± 2.4 & 75 (4)	-	-		
VI. CAM sampling	ESM removal	Y(Dettol®)	Y	Y (31G)	N	Y (S)	12.0 ± 3.1 & 55 (11)	13.5 ± 0.7 & 80 (10)	14.0 ± 0.9 & 90 (10)	13.6 ± 0.8 & 100 (9)	
	ESM removal + CAM pulling	Y(Dettol®)	Y	Y (31G)	Y	Y (S)	0.0 ± 0.0 & 0 (11)	12.22 ± 3.5 & 44 (9)	13.6 ± 1.2 & 42 (12)	13.8 ± 0.7 & 100 (8)	
	ESM removal + CAM sampling	Y(Dettol®)	Y	Y (31G)	Y	Y (S)	0.0 ± 0.0 & 0 (8)	12.5 & 11 (9)	11.9 ± 1.9 & 30 (10)	14.3 ± 0.8 &100 (8)	
	CAM sampling (surgical tools)	Y(Dettol®)	Y	Y (31G)	Y	Y (S)	0.0 ± 0.0 & 0 (10)	14.0 ± 2.2 & 60 (10)	0.0 ± 0.0 & 0 (8)	15.1 ± 0.8 & 100 (10)	
	CAM sampling (suction pen)	Y(Dettol®)	Y	Y (31G)	Y	Y (S)	0.0 ± 0.0 & 0 (8)	11.3 ± 0.7 & 22 (9)	0.0 ± 0.0 & 0 (8)	12.6 ± 0.9 &100 (8)	
	CAM sampling (micropipette)	Y(Dettol®)	Y	Y (31G)	Y	Y (S)	11.5 & 13 (8)	13.8 ± 1.9 & 25 (12)	13.1 ± 0.4 & 57 (7)	13.7 ± 0.9 &100 (22)	

ESM: Eggshell membrane; CAM: Chorioallantoic membrane; EtOH: Ethanol; BC: benzalkonium chloride; S: Silicone; C: Cyanoacrylate/Super glue; P: Paraffin; mm: millimetre; ED: embryonic day; Y: Yes; N: No; G: Gauge; and -: Not tested; n: Number of eggs per treatment: IC: Internal control; GC: Global control

Chapter 4: Proteomics

Evolution of the chick embryo chorioallantoic membrane proteome during early development

Sofhian Ali [1], Tamer A. E. Ahmed [1], Agrima Shrestha[1], and Maxwell T. Hincke [1,2,]

[1]Department of Cellular and Molecular Medicine, Faculty of Medicine, University of Ottawa, Ontario, K1H 8M5, Canada.
[2]Department of Innovation in Medical Education, Faculty of Medicine, University of Ottawa, Ontario, K1H 8M5, Canada.

Author's name:
Sofhian Ali
Tamer A. E. Ahmed
Agrima Shrestha
Maxwell T. Hincke

Corresponding authors:
Maxwell T. Hincke

This chapter corresponds to a manuscript accepted by the Journal of ACS Omega

Abstract:

In avian species, the chorioallantoic membrane (CAM) is a vital, highly vascularized extraembryonic structure that supports embryonic respiration, calcium transport and innate immune defence. In this study, we applied LC/MS/MS-based proteomics to CAM tissue harvested at embryonic days (ED) 6, 8, 10, and 12 to characterize its protein profile during the expression of different CAM functionalities during embryonic development and gain insight into possible sex-based distinctions. A total of 2,688 proteins were identified, with 2,347, 2,265, 2,351, and 1,267 proteins detected at ED 6, 8, 10, and 12, respectively. Notably, 1,191 common proteins were identified across all stages, while 124, 47, 86, and 2 proteins were uniquely expressed at ED 6, 8, 10, and 12, respectively. Functional annotation revealed correlations with abundant CAM protein constituents (as per their emPAI); for example: calcium mobilization - v-type proton ATPase subunit E1 (ATP6V1E1) and G1 (ATP6V1G1); intracellular transport - calcium-binding protein 39 (CAB39); vascular system & gaseous exchange - annexin A2 (ANXA2); lymphatics - actin, gamma 1 (ACTG1); blood elements - hemoglobin subunit alpha-1 (HBA1); immune defence – cathelicidin-1 (CATH1), cathelicidin-2 (CATH2); and protection against luminal toxic contents - thioredoxin (TXN). Notably, a sex-specific analysis identified 614, 320, 314, and 212 proteins that were uniquely expressed in female embryos, and 212, 273, 144, and 56 proteins only in male embryos at ED 6, 8, 10, and 12, respectively. The identification of sex-linked proteins during early CAM development may lead to an understanding of their functional roles and highlight the CAM's potential as a target for the development of *in-ovo* sex identification technology.

1. Introduction:

CAM structure and functions:

Avian species are important research models for studying disease, angiogenesis, and tumorigenicity (Ribatti et al., 2021; Ahmed et al., 2022). The chorioallantoic membrane (CAM) is a highly vascularized and multifunctional extraembryonic membrane which plays a vital and integral role in embryonic growth and development (Gabrielli & Accili, 2010; Nowak-Sliwinska et al., 2014). The CAM's multiple functionalities and rapid development, as well as accessibility, offer a highly advantageous platform (Nowak-Sliwinska et al., 2014). The CAM plays a pivotal role in regulating gas exchange (blood vessels), mediating calcium mobilization and intracellular transport (Gabrielli & Accili, 2010), contains a fully functional lymphatic system (Nowak-Sliwinska et al., 2014), and defends against pathogenic and toxic agents (antibacterial) (Ahmed et al., 2022; Cordeiro & Hincke, 2016). Table 4.1 illustrates the critical developmental phases of CAM as the embryo progresses over time. Embryonic growth associated with the CAM are seen in the establishment of the germ layer, which is the onset of CAM formation, following the partial fusion of three tissue layers between ED 5-6: the outer chorion, a central mesodermal layer which is rich in blood vessels, and an inner allantois membrane, followed by critical vascular expansion (Figure 4.1 and Table 4.1), with further development to attach to the inner eggshell membrane (ESM) (Nowak-Sliwinska et al., 2014). The progressive expansion and coordinated development of the chicken embryo and its CAM represent a series of intrinsic and extrinsic developmental events essential for embryogenesis (Nowak-Sliwinska et al., 2014). By ED 11–12, the CAM fully encloses the embryo, signifying the onset of the completion phase, during which structural and functional maturation of the extraembryonic membranes is achieved (Gabrielli & Accili, 2010; Lindgren et al., 2010; Makanya et al., 2016). At this stage, the vascular system undergoes extensive

remodelling and expansion, culminating in the formation of a highly organized vascular plexus. This dense network of capillaries facilitates efficient respiratory gas exchange and simultaneously establishes a primary barrier of innate immune defence against microbial pathogens (Nowak-Sliwinska et al., 2014). Thus, the completion phase represents a critical developmental transition, ensuring the embryo's survival and preparation for subsequent growth, leading to the emergence phase. At emergence, the CAM has reached peak vascular expansion and then degenerates as it is no longer needed, while the embryo has matured enough to hatch (Nowak-Sliwinska et al., 2014; Ahmed et al., 2022) (Table 4.1).

CAM, Embryo Sex Prediction and Proteomics:

The CAM's accessible nature and rich capillary network make it a valuable model for molecular investigations and *in vivo* research. LC/MS/MS-based proteomics can aid in identifying developmental biomarkers, which may also reflect the sex of the embryo. In birds, a homozygous ZZ genotype results in a male, while the female (hen) has a heterozygous ZW genotype (Bellot et al., 2017). A small number of sex-linked proteins, such as the SWIM-type zinc finger domain-containing protein (SWIM), are encoded solely by the W chromosome (He et al., 2019). Therefore, an analysis that confirms the presence or absence of W chromosome-encoded proteins could predict embryo sex. Previous work (Ahmed et al., 2022) has identified CAM proteins and conducted functional bioinformatics analysis of the mature CAM's functional role at ED12 and ED19 of the developing embryo. The primary goal of the current study was to identify the protein constituents of the CAM at early time points (ED6, 8, 10 and 12) in both female and male embryos using a LC/MS/MS-based proteomics approach and investigate their association with development of key functional CAM pathways, including calcium mobilization, intracellular transport, defense

against pathogen and luminal toxins, and lymphatics and vascular system development. Embryo sex was unambiguously determined using quantitative polymerase chain reaction (qPCR) of brain tissue to detect the W-specific SWIM gene (He et al., 2019), thereby further refining our analysis of proteomic results on a sex-specific basis. These sex-specific molecular insights into chick embryo developmental biology may pave the way for novel therapeutic strategies and diagnostic tools, offering a versatile platform for *in-ovo* sex prediction.

2. Materials and methods:

2.1 Egg Incubation and Candling

Fertilized White Leghorn eggs were obtained from the Canadian Food Inspection Agency (CFIA, Nepean, Ontario) and incubated in a Petersime Model 1 incubator (Petersime Incubator Co., Gettysburg, Ohio) with the broad end facing up. Eggs were candled (Titan Incubators, Malmesbury, England) on ED 0 to detect and eliminate any cracked or unfertilized eggs. No ethical approval was required for the *in-ovo* assessments, as all experimental groups and controls were terminated at ED16 by euthanization of embryos (Süß et al., 2023). All equipment was cleaned using 70% ethanol. Eggs were incubated until ED6, 8, 10, and 12, at which point the CAM and brain tissues were harvested and stored in Eppendorf tubes at -20 °C before molecular and proteomics studies. A total of 88 eggs were assessed during this study, of which 13 embryos yielded tissues that were subjected to proteomics analysis.

2.2 Sampling, Washing and Sonication of CAM

Whole CAM samples were collected from embryos on ED 6, 8, 10 and 12, using scissors and forceps, and stored at -20°C. CAM samples were washed by vortexing (Corning LSE,

Massachusetts, USA) with 1x buffered saline (PBS) (CAM to PBS ratio was 1:5), varying by volume of sample, and then centrifuged using an AccuSpin Micro 17R (Fisher Scientific) (5000 RPM, 5 minutes, 4°C). The supernatant containing residual egg yolk and egg white was removed. This step was repeated twice. The washed CAM samples were sonicated in 1x PBS at a 1:1 ratio using a Sonicator (Qsonica, Connecticut, USA) (40% amplitude, 1 minute, with 3-second on and 2-second off intervals). Sonicated CAM samples were then stored at -20°C until further analysis.

2.3 Sampling, Washing and Purification of Brain Tissue

For purification and isolation of Genomic DNA, the Wizard Genomic DNA Purification Kit (Promega) was used, following the manufacturer's protocol designed for the isolation of gDNA from Tissue Culture Cells and Animal Tissue. Briefly, whole brain tissue was collected from the same embryo used to collect whole CAM. Brain tissue (20 mg) was washed with the kit nuclei lysis solution (1:5 ratio of brain to nuclei lysis) by vortexing and then centrifugation (5000 RPM, 5 minutes, 4°C). The tissue was homogenized using the Qsonica Sonicator in the nuclei lysis solution. gDNA was extracted following the kit user manual and stored at 4°C overnight. Quality assessment and quantification of the purified DNA samples were performed using a NanoDrop 2000 Spectrophotometer, where the DNA concentration and absorbance ratios (A_{260}/A_{280} and A_{260}/A_{230}) were determined.

2.4 Protein concentration of CAM samples

The protein concentration of CAM samples was measured using the Bicinchoninic acid (BCA) assay (Thermo Scientific Pierce BCA Protein Assay), with bovine serum albumin as the standard. Samples and standards (25 µL) were prepared in a 96-well plate and mixed with 200 µL of BCA

working reagent, then incubated at 37°C for 30 minutes. Absorbances at 562 nm and 600 nm were measured using an Eon Microplate Spectrophotometer (BioTek) in dual wavelength mode.

2.5 Molecular sexing using polymerase chain reaction (qPCR)

Quantitative Polymerase chain reaction (qPCR) was used to identify the sex of embryos from which CAM tissue was also collected for subsequent proteomics. qPCR was performed in a 96-well PCR plate using CFX96 Real-Time PCR instrument (BioRad 1000 Alfred Nobel Drive, Hercules, CA 94547, United States) in a 20 µL reaction volume containing iQ SYBR green supermix (10 µL), cDNA template (75 ng, variable), 0.3 µM forward and reverse primers (2.4 µL), and DNase/RNase-Free distilled water. cDNA (25 ng/µL, variable) was amplified using specific primers for SWIM (a W-encoded, female-specific gene) and 12S (a housekeeping gene). Primers were specific for the W-encoded gene SWIM (SWIM-F: GAGATCACGAACTCAACCAG, SWIM-R: CCAGACCTAATACGGTTTTACAG) and the 12S ribosomal subunit (12S-F: CTATAATCGATAATCCACGATTCA, 12S-R: CTTGACCTGTCTTATTAGCGAGG) (He et al., 2019). Primer stocks were 100 µM, while working dilutions of 5 µM were prepared for PCR reactions. For PCR, an initial denaturation step was performed at 95°C for 3 min, followed by 35 cycles comprising DNA denaturation at 95 °C for 10 s, annealing at 57.3°C for 20 s, and extension at 72°C for 30 s. The melting curve analysis involved an increment of 0.5°C every second/step from 55 to 95°C. ΔCt values were used to calculate relative gene expression. Target gene expression was compared with that of the housekeeping gene 12S in terms of relative gene expression (He et al., 2019). Sex assignment was performed using the SWIM/12S ratio. The predictive criteria were as follows: a ratio (ΔC_q SWIM / ΔC_q S12) $\geq$ 2.0 indicated a male (absence of the W chromosome), while a ratio $\leq$ 1.5 indicated a female.

2.6 LC/MS/MS-based proteomics analysis

Suspended CAM samples were submitted to the Proteomics Platform of the Eastern Quebec Genomics Centre (Laval, QC, Canada) for LC/MS/MS analysis. Peptide separation was performed using reversed-phase (RP) nanoscale capillary liquid chromatography (nanoLC), coupled to an Agilent 1200 nanopump and an AB Sciex 5600 mass spectrometer (Framingham, Massachusetts, USA), equipped with a nanoelectrospray ionization source. Data acquisition (ES-MS/MS) was conducted using Analyst software (Version 1.6, AB Sciex, Framingham, Massachusetts, USA). MS/MS peak lists were generated using Protein Pilot (Version 4.5, AB Sciex, Framingham, Massachusetts, USA) and interrogated against the REF_GGallus_cUP000000539_20220913_20220913.fasta; contaminants_thegpm_20200924 database (unknown version, 27599 entries) using Mascot (Version 2.4.0, Matrix Science, London, UK) and X! Tandem (CYCLONE version, 2010.12.01.1). Search parameters specified carbamidomethylation of cysteine as a fixed modification and included deamidation (NQ), N-terminal glutamine to pyroglutamate conversion (Gln→pyro-Glu), and oxidation (Met, Pro) as variable modifications.

2.7 Protein identification

Proteomic datasets were analyzed and validated using Scaffold (version 5.3.3, Proteome Software Inc., Portland, OR, USA) against the NCBI Chicken database (http://www.ncbi.nlm.nih.gov/protein). Sequence validation employed BLASTP searches of non-redundant protein sequences using FASTA inputs, with confirmation based on query coverage, E-value, and Percent identity metrics. Redundant and contaminant proteins (i.e., human keratins) were excluded to refine the final inventory. Peptide identifications were accepted at ≥95%

probability, and protein identifications were filtered at a 1% false discovery rate (FDR) at both peptide and protein levels, requiring at least one unique peptide, with emphasis on unique peptide count. To serve as a false positive control, a total of 41 decoys were used, allowing for validation of the analysis.

2.8 Bioinformatics analysis

Gene ontology (GO) terms for proteins identified in the CAM (days 6, 8, 10, and 12; male and female embryos) were determined using DAVID functional annotation, and Bioinformatics Microarray Analysis (https://davidbioinformatics.nih.gov/summary.jsp) for the clustering tables, with P-value significance as the basis for clustering ($P \leq 0.05$). Cluster numbers with corresponding functional GO terms are identified for tables to compare common male-female functions, as well as unique female and unique male functional annotations at each time point: ED 6, 8, 10, and 12. Each GO term corresponded to an EASE score (a modified Fisher Exact P value and high enrichment value), using GOTERM_BP. An enrichment score of less than (EASE<1.0) was discarded from the functional annotation analysis. DAVID Bioinformatics Resources was also used for pathway mapping of the entire protein list via Kyoto Encyclopedia of Genes and Genomes (KEGG) enrichment analyses (https://bioinformatics.sdstate.edu/go/) (Ahmed et al., 2022), with a threshold of $P < 0.05$. Kyoto Encyclopedia of Genes and Genomes (KEGG) Pathway dot graphs were generated from the website. Enrichment analyses with a threshold of FDR <0.05 for the P values and 25 pathways shown. Venn diagrams were generated using PowerPoint, and protein analysis was conducted in Excel. All figures were generated using the Microsoft Office package, including PowerPoint and Excel, along with the open-source software GIMP (version 2.10) and Adobe Photoshop CS version 8.0.

3. Results

The structural expansion of the CAM during development is depicted in figure 4.1, which shows images of fertilized White Leghorn eggs photographed under a high-intensity candler at time points ED 6, 8, 10, and 12. A developing vascular system is observed, as the yellow hue turns red with increased growth of blood vessels. Comprehensive analysis of the CAM proteomics data identified its protein constituents at various early developmental time points: ED 6, 8, 10, and 12. Further analysis was conducted by identifying unique and common proteins for female and male embryos at these time points. A total of 13 CAM tissue samples were extracted and processed for analysis at the Université Laval proteomics platform, comprising 3 of ED6 samples (2 females, 1 male), 4 of ED8 samples (2 females, 2 males), 4 of ED10 samples (2 females, 2 males) and 2 of ED12 samples (1 female and 1 male), with sex determined using qPCR to verify the presence or absence of the W-encoded SWIM gene (methods). The temporal distribution of identified common and unique CAM proteins during early development of the chick embryo is shown in figures 4.2 and 4.3. A total of 2688 proteins were identified (Table S1) in the final inventory dataset. Raw and level 1 datasets were deposited on the cloud-based communal Mendeley repository (https://data.mendeley.com/datasets/967dc5z8tv/1). Figure 4.2, panel A, shows a compound Venn diagram displaying the distribution of identified unique and common proteins at ED 6, 8, 10, and 12. Unique proteins identified in the compound Venn diagram at ED6, 8, 10 and 12 were 124, 47, 86 and 2, respectively, with 1,191 proteins being common to all time points (Figure 4.2A). Further analysis of proteins uniquely identified at each time point using KEGG pathway analysis revealed various functional pathways, with 9, 0, 1, and 1 pathways identified at ED6 (Figure 4.2B), ED8, ED10 (Figure 4.2C), and ED12 (Figure 4.2E), respectively. In addition, KEGG pathway analysis of proteins common to all time points revealed 25 various functional pathways (Figure 4.2E). This

enrichment analysis highlights significant pathways based on common and specific biological processes across different time points, showcasing pathways that are both common and specific to biological processes. Further analysis generated data segregating unique and common proteins between male and female embryos at various time points, ED 6, 8, 10 and 12 (Figure 4.3). The total number of proteins identified in the CAM tissue samples was 2,347, 2,265, 2,351, and 1,267 for ED6, 8, 10, and 12, respectively. At ED6, 2,347 proteins were identified, with 2,135 in females and 1,733 in males; 614 were female-specific, 212 male-specific, and 1,521 shared. At ED8, 2,265 proteins were found (1,992 female, 1,945 male), with 320 female-specific, 273 male-specific, and 1,672 common. At ED10, 2,351 proteins were identified (2,207 female, 2,040 male), including 311 female-specific, 144 male-specific, and 1,896 shared. At ED12, 1,267 proteins were detected (1,211 female, 1,055 male), with 212 female-specific, 56 male-specific, and 999 common (Figure 4.3). KEGG enrichment analysis was also performed for proteins identified at different time points (ED 6, 8, 10, and 12) for both male- and female-specific CAM samples to identify significant functional pathways. Figure 4.4 illustrates the enriched pathways for the four developmental timepoints: ED 6, 8, 10, and 12. The first panel displays significant pathways for female-specific proteins, the second panel shows male-specific pathways, and the third panel illustrates the commonalities of significantly enriched pathways shared by both male and female samples. For ED6, all panels displayed 25 significantly enriched pathways, with some panels having a high number of proteins (>50) identified for certain biological processes. KEGG analysis of proteins identified in ED8 showed 25 significantly enriched pathways for all panels. KEGG pathway analysis of proteins identified at ED10 revealed 25 significant pathways specific to females and common to both sexes, while for male-specific proteins, only 3 significant pathways were identified. KEGG pathway analysis of proteins identified at ED12 revealed 25 significant

pathways specific to females, 25 significant pathways common to both females and males, and 18 significant pathways specific to males. The most enriched pathways include cellular component organization, which is highly enriched at ED 6, 8, and 10. In addition, a protein-containing complex was highly enriched in the small molecule metabolic process, especially at ED6, while the organonitrogen metabolic process is observed at ED8 and ED12. The signaling pathway is particularly prominent at ED10 in male samples, where it is one of only three pathways identified. Functional insight was obtained using DAVID bioinformatics tools, which identified functional annotations of specific proteins at different time points. Functional annotation analysis was also conducted for sex-specific and common proteins using Gene Ontology (GO) term enrichment analysis. Table 2 summarizes the protein families identified in the proteomics data across various time points. The main protein families identified in ED 6, 8, 10 and 12 include collagens, translation initiation factors, serpins, heat shock proteins, and heterogeneous nuclear ribonucleoprotein, along with heat shock, motor, and cellular death proteins. Table S2 presents the number of identified functional clusters, as determined by DAVID, based on common and unique proteins found in female and male CAM tissue samples. The total number of predicted functionalities for proteins identified at ED 6, 8, 10, and 12 was 20, 18, 21, and 17, respectively. All DAVID analyses of functionalities were subjected to a cut-off criterion of the enrichment score (EASE < 1.0), ensuring that only pathways and biological processes with statistically meaningful enrichment were included in functional interpretation. The carbohydrate metabolic process (GO:0005,975) exhibited the highest number of proteins across different time points: ED 6 (32), ED 8 (30), ED 10 (33), and ED 12 (23), reflecting the importance of synthesizing and converting carbohydrates to provide energy and build structural components during embryonic development. The tricarboxylic acid cycle (GO:0006,099) functionality was also highly enriched across

developmental time points, with multiple proteins identified at ED 6 (24), ED 8 (23), ED 10 (25), and ED 12 (23). Other highly enriched functionalities include the translation initiation factor activity (GO:0,003,743), which is highly enriched in ED 6 (26) and ED 10 (30) proteins. barbed-end actin filament capping (GO:0,051,016 barbed-end actin filament capping) identified in ED8 (12) proteins. The unfolded protein binding (GO:0,051,082) and ATP hydrolysis activity (GO:0,016,887) are enriched in ED12, with 30 and 25 proteins identified as related to these functional roles, respectively. Enriched functionalities identified in female samples at ED6 include autophagy (GO:0.006914, 7 proteins) and hyaluronic acid binding (GO:0.005540, 5 proteins), while at ED8, phosphatidylcholine transporter activity (GO:0.008525, 3 proteins) was identified. In addition, autophagy (GO:0,006,914, 5 proteins) was identified in female samples at ED10. Figure 4.5 illustrates a functional mapping diagram of the various CAM samples and their associated proteins, indicating the significant roles of these proteins in CAM at various time points for each sex. Figure 4.6 presents a heatmap of 177 proteins identified as the most important functional constituents of CAM development among the total CAM proteome (2,688 proteins). These proteins have roles in structural integrity, signalling, and metabolic processes, and are hierarchically categorized based on their abundance (emPAI values). On the other hand, table S3 lists the top 100 most abundant protein constituents in the entire proteomics dataset, as per their emPAI values. Among these, 48 proteins are also identified in the heatmap (Figure 4.6). The heat map revealed clear trends in protein abundance across ED 6–12. Among the highest expressed proteins were structural and metabolic proteins such as hemoglobin subunits alpha 1 (HBA1), alpha D (HBAD), beta A (HBBA), epsilon (HBE), beta R (HBBR), zeta (HBZ), and epsilon 1 (HBE1), which consistently showed emPAI values in the upper ranges (5-10 to >500), reflecting their dominant roles in oxygen transport and nutrient supply during development. In contrast, the

lowest abundance proteins were specialized regulatory or signalling proteins such as ferrochelatase (FECH), fibrinogen beta chain (FGB), fibrinogen gamma chain (FGG), G protein subunit alpha Q (GNAQ), heme oxygenase 1 (HMOX1), heme oxygenase 2 (HMOX2), cytochrome P450 family 2 subfamily C member 18 (CYP2C18), calbindin 1 (CALB1), integrin alpha 9 (ITGA9), galectin 2 (LGALS2), mitochondrial calcium uptake 2 (MICU2), myoferlin (MYOF), phospholipase C gamma 1 (PLCG1), protein O-fucosyltransferase 1 (POFUT1), protein O-fucosyltransferase 2 (POFUT2), protein phosphatase 3 catalytic subunit alpha (PPP3CA), proteasome 26S subunit ATPase 1 (PSMC1), proteasome assembly chaperone 1 (PSMG1), serpin family B member 5 (SERPINB5), stromal interaction molecule 1 (STIM1), sulfotransferase family 1E member 1 (SULT1E1), tubulin beta 6 class V (TUBB6), and vitelline membrane outer layer 1 homolog (VMO1), which appeared in the lowest emPAI category (0–0.25 to 0.5–1). Figure 4.7 presents the functional categorization of 52 chicken proteins associated with angiogenesis. Protein groups are classified in major functional categories; ECM components, including collagens (COL1A1, COL1A2, COL4A1, COL4A2, COL6A13), laminins (LAMA5, LAMB2, LAMC1), nidogens (NID1, NID2), and fibronectin (FN1), were detected, highlighting a robust basement membrane structure supporting endothelial cell attachment and vessel stabilization. Proteins associated with cytoskeletal dynamics and cell–matrix interactions, such as ITGA1, ITGA9, ITGAV, ITGB1, ITGB3, VCL, ACTG1, and TLN1, were also identified, suggesting endothelial migration and sprouting. Antioxidant and metabolic regulators (SOD2, PRDX3,4 and 6, GPX1, HMOX1 and 2) are consistent with high metabolic demand and oxygen-regulated vessel growth. Collectively, the protein profile demonstrates a microenvironment optimized for rapid vascular expansion, consistent with CAM development between ED6–12. This perspective illuminates how structural, metabolic, and regulatory factors coordinate the progression of angiogenesis. Each protein group

is associated with key angiogenic stages: endothelial activation, ECM degradation, sprouting, migration, and tube (lumen) formation. The general trend indicates that core structural, transport, and metabolic proteins dominate CAM proteomic profiles, while enzymes, modulators, and signalling proteins remain at lower abundance during development.

4. Discussion

The chick embryo CAM is a popular vascularized model used in various biomedical studies due to its rapid growth and accessibility (Nowak-Sliwinska et al., 2014). The CAM is extensively used in angiogenesis, tumour graft, drug delivery and toxicity studies (Chen et al., 2021). The CAM is the avian homolog of the mammalian placenta (Lindgren et al., 2010; Makanya et al., 2016), as both extraembryonic tissues carry out a wide array of similar functions essential for embryo viability, growth, and development. The highly vascularized CAM tissue begins to develop after the fusion of the allantois with the chorion between days 5 and 6 and surrounds the embryo by ED11-12 (Ribatti, 2017; Gabrielli & Accili, 2010). This study provides an extensive proteomic characterization of the chick embryo CAM across early developmental time points. The selected four timepoints (ED 6, 8, 10, 12) encompass the early formation and maturation of the CAM, while previous CAM proteomic studies with white Leghorn embryos have focused on the fully functional CAM at ED 12 and 19 (Ahmed et al., 2022; Cordeiro and Hincke, 2016), or in specialized breed of Tibetan chickens at ED 6, 10, 14 and 18 (Zhang et al., 2020). The time course of expression of the CAM proteome from male and female embryos may have specific differences, in addition to many common proteins, that reflect sex-specific functionalities or differences in their developmental rates, since male embryos develop faster (Tagirov & Golovan, 2015). To gain further insight into the underlying complexity of CAM contribution to embryonic growth and

development, sex-specific protein expression was therefore investigated concerning the main functions of the CAM: gaseous exchange (blood vessels), blood elements and calcium mobilization (Gabrielli & Accili, 2010), lymphatics (Nowak-Sliwinska et al., 2014), and pathogenic and toxic content defence (antibacterial) (Ahmed et al., 2022; Cordeiro & Hincke, 2016). To better understand the functional and physiological complexity of CAM, we sought to establish a proteomic foundation for the essential functions associated with development and to identify potential sex-linked differences. The CAM fulfills several primary functions that integrate ancillary roles within a broader framework. The roles of the CAM's molecular constituents underpinning embryonic development were elucidated, with a focus on the vascular system, calcium transport, and defence against pathogens and toxic agents.

4.1 Proteomic features of the CAM vascular system during development

4.1.1 angiogenesis

The chick embryo vascular system is essential for development, and it is a crucial constituent of the CAM. The vascular system supports the embryonic life of a chick embryo (Moreno-Jiménez et al., 2016). In the early stages of embryonic life, starting from ED (3-5), the embryo undergoes morphogenesis (Sarnella et al., 2024), during which most of the organs and functions begin to form and establish baseline activities for further growth. Thus, vascular system formation is initiated, the heartbeat commences, and limb development progresses, culminating in the emergence of wings and legs. (Tong et al., 2013). The formation of the CAM begins as early as ED 4, and by ED 5-6, the CAM has started to conduct gaseous exchange, and vascular network expansion begins as it is established but not yet mature (Table 4.1) (Chen et al., 2021; Deryugina & Quigley, 2008) (Table 4.1). In our proteomics study, numerous proteins associated with the

gaseous exchange and the development of the small capillary network of thin vessels were identified, as shown in figures 4.5 and 4.6. Proteins in the annexin superfamily (A1, A2, A5, A7, A8-like 1) (Table 4.2) are among the proteins identified. A similar proteomic study conducted by Ahmed et al. (2022) also identified the same annexin family members in the CAM tissue samples at ED12 and ED19. The annexins are particularly important in cell signalling, membrane repair, and structural development, as well as their roles in Ca^{2+} transport. Studies have shown that annexins are involved in angiogenic activity, either by reducing or increasing angiogenesis (Lokman et al., 2013; Pin et al., 2012). In the current study, annexin A2 is a highly abundant protein (Figure 4.6), compared to the other proteins listed for the blood vessel category in figure 4.5, with ED6 and ED12 showing higher levels than ED8 and ED10. Similarly, other proteins, such as but not limited to nidogen (1 and 2) are important for ECM development, decorin, malate dehydrogenase 2, aconitase 2, peroxiredoxin (3, 4, and 6), and glutathione peroxidase 1, are related proteins involved in CAM vascularization, which have roles in metabolic reactions, signalling and as transporters can occur directly or indirectly. Other identified proteins including, protein cytochrome C, somatic (CYCS), laminin subunit (beta-2, alpha-5, gamma-1), catenin (alpha-1 and beta-1), and ubiquinol-cytochrome c reductase core protein 1 (UQCRC1), the collagen protein family (collagen subunits 1a1, 1a2, 3a1, 4a1, 4a2, 5a2, 6a1, 6a2, 6a3, 11a1 and 12a1), were seen associated with GO:0,005,201 extracellular matrix structural constituent functional DAVID cluster, fibulin (1 and 2), and integrin subunit (alpha-V, beta-1, alpha-9, alpha-1, beta-3). The detected protein network reflects the CAM's highly angiogenic nature during these developmental stages. Figure 7 underlines the relationship between angiogenic proteins and vascular formation. Structural ECM proteins (collagens, laminins, and nidogens) reflect the mature yet dynamic basement membrane that provides a scaffold for endothelial sprouting. Their interaction with

integrins (ITGA1, 9, V, ITGB1, and 3) supports coordinated cell adhesion, migration, and capillary branching. Figure 7 also highlights redox regulators (PRDX 3, 4 and 6, HMOX1,2, SOD2), which play a protective role against endothelial damage during the oxidative stress associated with rapid vascular growth and the increasing metabolic demands of the embryo. Catenin beta-1 was also identified in the study by Soulet et al. (2013) in chick embryo intestinal tissue at ED16. Thus, the catenin beta 1 is a canonical signalling pathway associated with tissue regeneration (Zhang et al., 2008; Soulet et al., 2013). Fibulins play important roles in tissue remodelling, basement membrane, and elastic fibre structural integrity (Mahajan et al., 2021). Integrins, a family of heterodimeric transmembrane proteins, mediate cell adhesion to the extracellular matrix. Integrin subunits can heterodimerize in at least 20 different combinations (Eliceiri & Cheresh, 1998). A study suggests that the integrin protein (alpha V-beta 3) combination of those subunits may have a role in angiogenetic activity in CAM, are proteomics has identified both subunits (Eliceiri & Cheresh, 1999). Studies suggest that CAM modulates the composition of collagen type IV, fibronectin, laminin, and glycosaminoglycan-associated proteins, promoting angiogenesis (Ribatti, 2016; Chen et al., 2021; Ahmed et al., 2022). It has been demonstrated that CAM extracts exhibit enzymatic activity capable of degrading type IV collagen (Missirlis et al., 1990). This protein landscape explains why CAM is widely used as an *in vivo* angiogenesis model, as highlighted by the results of this proteomics study.

4.1.2 Hematopoiesis and plasma protein biosynthesis

Our proteomics study identified key blood proteins of the CAM. These include hemoglobin subunit beta-A (HBBA), beta-R (HBBR), alpha-1 (HBA1), delta (HBAD), epsilon-like (HBE/HBE1), and zeta-globin (HBZ) (Ahmed et al., 2022). These proteins are the most abundant,

as shown in our heatmap (Figure 4.6), where most blood proteins exhibit an emPAI > 500. These proteins were most abundant at ED8 and ED12. Iron homeostasis is supported by the expression of transferrin receptor (TFRC) (Wang et al., 2020), transferrin (TF), and ferritin heavy chain 1 (FTH1), especially noted at days 6 and 8. ALB (albumin), the most abundant protein in the blood plasma (Dakhel et al., 2021), alpha-2-macroglobulin (A2M), and protein Z-dependent protease inhibitor (SERPINA10) are expressed across the time points, most prominently at day 6 and 8, supporting protease inhibition and nutrient transport functions in the developing vascular system within the blood. Coagulation factors, such as F2 (thrombin), have been shown to promote angiogenesis in the developing CAM (Tsopanoglou et al., 1993; Caunt et al., 2003). In contrast, von Willebrand factor (VWF) is a procoagulant that mediates platelet aggregation (Mojiri et al., 2016). Although FGA, FGB and FGG were detected in the proteomic profile, their comparatively low emPAI values suggest limited relative abundance within the sample proteome.

4.1.3 Lymphatic system

Lymphatics are another important component of the vascular system. The CAM has a similar lymphatic system to that of a mammalian lymphatic system (Nowak-Sliwinska et al., 2014), and our study offers insights into lymphangiogenic activity occurring from day 6 to day 12 of embryonic development. Lymphatics are first noticeable in chick embryos at ED 4-5 (Clark and Clark, 1919), whereas lymphangiogenesis begins at ED 5–9 (Ribatti, 2025; Nowak-Sliwinska et al., 2014). Some of the proteins identified in our study and are involved in lympahtics development, include desmoplakin (DSP), mitogen-activated protein kinase 3 (MAPK3), PDZ and LIM domain protein 3 (PDLIM3), proteasome assembly chaperone 1 (PSMG1), mannose receptor C Type 2 (MRC2), junction plakoglobin (JUP), neuropilin-1 (NRP1), myoferlin (MYOF),

collectin subfamily member 12 (COLEC12), vascular endothelial, cadherin (CDH5), actin, gamma 1 (ACTG1), myosin heavy chain 9 (MYH9), myosin light chain 12A (MYL12A), filamin A (FLNA), vinculin (VCL), vimentin (VIM), talin-1 (TLN1), integrin-linked kinase (ILK), vascular cell adhesion molecule 1 (VCAM1), fibronectin 1 (FN1), secreted protein acidic and rich in cysteine (SPARC) and periostin (POSTN). The heatmap reveals a coordinated molecular signature comprising endothelial-specific adhesion molecules (VCAM1, CDH5/VE-cadherin) mediating leukocyte adhesion and junctional integrity (Gurtner et al., 1995), desmosomal components (JUP/plakoglobin, DSP/desmoplakin) establishing intercellular adhesion complexes for vascular and lymphatic stabilization (Yuan et al., 2021), cytoskeletal regulators (ACTG1, VCL, VIM, TLN1) facilitating motility and morphological remodeling (Nowak-Sliwinska et al., 2010), extracellular matrix effectors (FN1, SPARC) driving ECM restructuring for endothelial migration and vessel morphogenesis (Brekken & Sage, 2000; Chen et al., 2021), collagen receptor MRC2 promoting ECM degradation during lymphatic sprouting (Miura et al., 2023), and signaling receptors (NRP1, COLEC12) implicated in VEGF-mediated endothelial specification, vessel organization, and innate immune-like activity (Riley & Bradshaw, 2020; Rivera et al., 2011), collectively delineating a dynamic yet tightly orchestrated transition from an actively migratory to a vessel-maintenance phenotype that underpins regulated lymphangiogenic and vasculogenic patterning during embryonic CAM development.

4.2 Ca^{2+} Transport

The CAM plays a pivotal role in mobilizing calcium from the eggshell (ES) and delivering it to the developing embryo for skeletal development (Ahmed et al., 2022). Calcium mobilization and transport are coordinated through carbonic anhydrases, ion transporters and calcium-binding

proteins. CAM proteomic analysis across ED 6-12 identifies many protein constituents involved in calcium-related functions.

Certain identified proteins in our study related to calcium mobilization include carbonic anhydrase II (CA2), XIII (CA13) and IX (CA9), v-type proton ATPase subunit E1 (ATP6V1E1) and G1 (ATP6V1G1), plasma membrane calcium-transporting ATPase 4 (ATP2B4) and sarcoplasmic/endoplasmic reticulum calcium ATPase 2 (ATP2A2), calbindin 1 (CALB1) and calreticulin (CALR), annexin A1 (ANXA1), A2 (ANXA2), A5 (ANXA5) and A6 (ANXA6), collagen type I alpha 1 chain (COL1A1), alpha 2 chain (COL1A2), type IV alpha 1 chain (COL4A1), type IV alpha 2 chain (COL4A2), fibrillin-1 (FBN1), lumican (LUM), decorin (DCN), matrix metalloproteinase-2 (MMP2), cathepsin K (CTSK), periostin (POSTN), tenascin C (TNC) and vitelline membrane outer layer protein 1 homolog (VMO1). The carbonic anhydrase isozymes are markers of the villus cavity cells of the ectodermal and endodermal epithelium; their expression is involved in CAM-mediated processes, such as calcium transport (Gabrielli et al., 2001). CAM carbonic anhydrase activity is correlated with calcium transport-related functions (Tuan & Zrike, 1978). Carbonic anhydrases catalyze the hydration of CO_2, generating protons that acidify the ES to promote calcium solubilization (Rieder et al., 1980; Anderson et al., 1981; Narbaitz et al., 1981; Tuan, 1984; Tuan et al., 1986; Halgrain et al., 2022). In our study, we identified low levels of CA2, CA13, and CA9 in the CAM proteome at ED 6, 8 and 10 (Figure 4.6), with emPAI values ranging from 0.25 to 1 and at ED12, not detectable for CA9. The presence of these proteins correlates with the presence of ATP-driven ion pumps, including the ATP6V1E1 and ATP6V1G1 proteins, which are constituents of the vacuolar H^+-ATPase (V-ATPase) complex. This complex further facilitates proton transport into the (ESM/ES) interface (Halgrain et al., 2022; Ahmed et al., 2022). Expression of extracellular matrix (ECM) components, such as COL1A1, COL1A2, COL4A1,

COL4A2, FBN1, and DCN, as well as LUM, contributes to the extracellular matrix structure of the CAM. Periostin (POSTN) and tenascin C (TNC), both involved in osteogenic ECM dynamics (Wasik et al., 2022). Calcium mobilization from the eggshell is a crucial process facilitated by the CAM, which enables the solubilization of calcium ions necessary for embryonic growth and skeletal development.

Intracellular calcium transport in CAM cells is tightly regulated by several distinct networks, which play a crucial role in delivering calcium through transport mechanisms during embryonic development. Proteomic analysis across ED 6 - 12 reveals key proteins for maintenance of calcium homeostasis, including protein S100-A11 (S100A11), sodium/potassium-transporting ATPase subunit beta-1 (ATP1B1), calcium-binding protein 39 (CAB39), calcineurin B homologous protein 1 (CHP1), sarcoplasmic/endoplasmic reticulum calcium ATPase 2 (ATP2A2), stromal interaction molecule 1 (STIM1 not detectable at ED12), calmodulin-1 (CALM1), protein S100-A10 (S100A10), and calcium/calmodulin-dependent protein kinase type II delta chain (CAMK2D). These proteins are listed in the heatmap (Figure 4.6), with moderate emPAI values. S100 family members and calmodulin-1 (CALM1), and calcium-binding protein 39 (CAB39) are calcium-binding proteins (Yáñez et al., 2012).

4.3 Innate Immune Defence

4.3.1 Defence Against Luminal Toxic Contents

The ES acts as the first line of defence against pathogens, and the CAM plays a role as the second line of defence (Hincke et al., 2019). The innermost layer of the CAM is the allantois, derived from a sac-like structure that emerges from the ventral wall of the endodermal hindgut. It is a

reservoir for metabolic waste (Ribatti, 2016). Our proteomic analysis, spanning ED6 to ED12, identifies CAM constituents that may play a significant role in protecting the embryo from luminal toxins. Our proteomics have identified several proteins related to barrier function, including heat shock proteins, protein 90 alpha family class B member 1 (HSP90AB1), heat shock protein 5 (HSPA5). Sulfotransferase proteins were also identified (SULT1B1, SULT1C3 and SULT1E1), as well as other proteins such as disulfide-isomerase (PDIA4 and PDIA6), cathepsin (CTSB and CTSK), and proteasome subunit alpha type-1 (PSMA1), beta type-1 (PSMB1), and 26S proteasome regulatory subunit (PSMC1). Alpha-L-fucosidase 2 (FUCA2), signalling protein Cell division control protein 42 homolog (CDC42), glycosylation enzymes Protein O-fructosyltransferase 1 and 2 (POFUT1 and POFUT2). Antioxidant enzymes superoxide dismutase (SOD1 and SOD2), catalase (CAT), the glutathione transferase family members kappa 1 (GSTK1), glutathione s-transferase alpha (GSTA2, GSTA3 and GSTA4) serve as important antioxidant enzymes for protection in the chick embryo (Yang et al., 2018), and the redox regulators peroxiredoxin (PRDX1, PRDX4 and PRDX6), thioredoxin (TXN), thioredoxin domain-containing protein 5 (TXNDC5), and glutathione peroxidase 1 (GPX1). Detoxification proteins include cytochrome P450 2C18 (CYP2C18), aldehyde dehydrogenase family member 1A1 (ALDH1A1), and aldehyde dehydrogenase family member 5A1 (ALDH5A1). Specifically, protein 90 alpha family class B member 1 (HSP90AB1) and glycosylation enzymes FUCA2 (fucosidases), POFUT1 and POFUT2 (fucosyltransferases) are the main enzymes involved in the incorporation and cleavage of L-fucose residues (Tu et al., 2013). Superoxide dismutases (SOD1/SOD2) are ubiquitous enzymes found in all aerobic organisms (Wang et al., 2018). The SOD proteins help to control reactive oxygen species, limiting toxicity and confer protection against oxidative stress (Wang et al., 2018). CAT catalyzes the dismutation of hydrogen peroxide to form the neutral

products water and oxygen (Yang et al., 2018). Glutathione s-transferase alpha (GSTA2 and GSTA4) both play a role in detoxification, and GSTA2 is highly important against oxidative stress in chick embryo (Tetlow & Board, 2004; Yang et al., 2018). Our gaseous environment inherently generates reactive oxygen species in biological tissues. To protect embryonic development, a robust redox defence system is crucial for maintaining barrier integrity. The thioredoxin-peroxiredoxin (TXN–PRDX) system balances the activity of hydrogen peroxide generated through mitochondrial cellular respiration (Habashy et al., 2021). The TXN protein is most abundant for this functionality across ED 6-12, with emPAI values ranging between 5 and 25. ALDH1A1 and ALDH5A1 belong to a family of aldehyde dehydrogenases that share similar functions with thioredoxin-peroxiredoxin, which are related to the control of oxidative stress and cell damage and represent additional detoxifying proteins in organisms that help control reactive oxygen species (Singh et al., 2013). Heat shock proteins were also identified in the CAM proteome, which play a crucial role in regulating protein folding and the stress response. DAVID-based functional annotation revealed functionality related to the embryo associated with heat shock protein roles, including GO:0.031,072 heat shock protein binding and GO:0.044,183 protein folding chaperone, at all timepoints (Table S2a, b, c, d and e). The cluster cell redox homeostasis (GO:0,045,454) was also identified (9 proteins), with most proteins belonging to the peroxiredoxin family (Table S2). In addition, the functional cluster thioredoxin peroxidase (GO:0,008,379) contains 3 proteins of the peroxiredoxin family.

4.3.2 Protection against pathogenic invasion

The exposure of the egg surface to microbes during natural incubation can expose the embryo to pathogenic agents that penetrate the eggshell; therefore, the egg possesses innate defence

mechanisms such as the physical and chemical barriers of the eggshell (Horrocks et al., 2014; Hincke et al., 2019). Moreover, internal to the eggshell and associated membranes, the CAM surrounds the developing embryo and contains antimicrobial proteins that reinforce those of the eggshell and egg white (Hincke et al., 2019). Our CAM proteomics study revealed several proteins related to defence against pathogens, including BPI fold-containing family B member 2 (BPIFB2), serine protease inhibitors serine peptidase inhibitor kazal type 5 (SPINK5) and serine peptidase inhibitor kazal type 7 (SPINK7), and cysteine protease inhibitors cystatin-B (CSTB) and cystatin-C (CST3) and cathelicidin-1 (CATH1), cathelicidin-2 (CATH2) proteins. The Serpin family is represented by serpin family B member 1 (SERPINB1), member 5 (SERPINB5), member 6 (SERPINB6), and serpin family H member 1 (SERPINH1), serpin family F member 1 (SERPINF1) and member 2 (SERPINF2). Lysozyme C (LYZ) and peptidoglycan recognition protein 2 (PGLYRP2), while the complement system includes complement C3 (C3) and complement factor H (CFH). The group of calgranulins & Lectins includes Protein S100A12 (S100A12) and galectin-2 (LGALS2), galectin-1A (LGALS1A) and galectin-1B (LGALS1B). Other important defence molecules are alpha-2-macroglobulin (A2M), high mobility group protein B1 (HMGB1) and beta-2-microglobulin (B2M), avidin (AVD), immunoglobulin lambda-like polypeptide 1 (IGLL1), ovalbumin-related protein Y (SERPINB14B) (OVALY), ovalbumin-related protein X (SERPINB14C) (OVALX), ovostatin (OVST), protein Ovotransferrin (TF), and protein vitellogenin-2 (VTG2). Ovalbumin (SERPINB14) (OVAL) is the most abundant protein across ED 6-12 for this functionality; although there is no direct evidence that it provides antimicrobial protection, ovalbumin can modify calcium carbonate crystallization and may play a role in eggshell calcification (Moreau et al., 2022). Many proteins associated with this function are present in different tissues of the developing embryo; for example, SPINK 5 and 7 are major

protease inhibitors of the egg white (Saxena & Tayyab, 1997). On the other hand, OVAL could serve as a nutritional source of amino acids for the embryo (Da Silva et al., 2015), while TF, identified in egg white and eggshell (Hincke et al., 2019), is involved in iron transport. The serpin class family proteins, comprising twenty-seven serpins belonging to clades A, B, C, D, E, F, G, H, and I, were identified within the chicken genome, participating in egg formation (Dombre et al., 2017). Increasing evidence suggests that the serpin family may play roles in cell proliferation, tissue remodelling, and/or angiogenesis, as well as eggshell biomineralization, egg defence, and embryo nutrition (Dombre et al., 2017; Ahmed et al., 2019). Similarly, several serpin proteins were identified at ED 12 and 19 in the CAM and embryonic blood, and eggshell membrane, such as SERPINs (SERPINB1, SERPINB2, SERPINB5, SERPINB10B, SERPINB6, SERPINB14B, SERPINB14C, SERPINH1 and SERPINE2) (Ahmed et al., 2022; Ahmed et al., 2019). The serpin B family is expressed in the hen reproductive tissues and exported into the egg during its formation, where they constitute major protein components in egg structures such as egg white, yolk and eggshell; three proteins were identified in our proteomics: SERPINB14 (OVAL), SERPINB14B (OVAY), and SERPINB14C (OVAX) (Dombre et al., 2017). SERPINB14C (OVAX) could participate in egg defence, since it is active against *listeria* and *salmonella* (Réhault-Godbert et al., 2013). CATH1 and CATH2 belong to the major class family of cathelicidin proteins. Studies suggest that both CATH1 and CATH2 are major antimicrobial agents (Wang et al., 2020). Antimicrobial activity is present in this class of proteins, such that they exhibited antimicrobial activity toward gram-positive and gram-negative bacteria (Wang et al., 2020). LYZ, OVST, and TF are also major antimicrobial proteins of the egg white and eggshell membrane (Dombre et al., 2017; Ahmed et al., 2019). A similar trend is observed for LYZ and TF proteins (Figure 4.6), where their abundance gradually increases as the embryo grows, (Figure 4.6). OVST has a stable

but low abundance across all timepoints studied (Figure 4.6). Other related proteins are detected at lower abundance across our study. The antimicrobial proteins identified in this CAM proteomics study provide a protective mechanism against pathogen invasion.

4.4 *In-ovo* sex prediction

At ED 5-6, the sexual reproductive organs and sex differentiation have been established (Tong et al., 2013) (Table 4.1). The early onset of sexual reproductive differentiation could lead to sex-based differences in gene expression and protein abundance (Hennequet-Antier et al., 2024). A focus of this study was to investigate a possible correlation between the expression of the CAM proteome and the embryo sex. Our proteomic analysis of chick CAM samples across ED 6-12 revealed sex-related patterns emerging during early development, suggesting that biological sex is associated with distinct CAM functionality during critical developmental windows. Such a difference could be related to the observation that male embryos develop faster than females in birds (Cook & Monaghan, 2004; Tagirov & Golovan, 2015). Across the studied time points (ED 6-12), female CAM samples consistently showed a higher number of unique proteins and enriched biological pathways compared to male samples (Figure 4.3). For example, at ED6, female samples displayed 614 unique proteins compared to 212 in males, while they shared 1,521 common proteins. Across all time points, our analysis revealed that female-based samples exhibited more functional relationships with specific proteins than their counterparts, as observed in our DAVID analysis; thus, more proteins were identified in female samples overall. At ED6, 2,135 proteins were assigned to female samples, and 1,733 proteins were assigned to male samples. Functional annotation using DAVID and Gene Ontology (GO) (Table S2a) revealed distinct processes, including autophagy (GO:0006914) and hyaluronic acid binding (GO:0005540) in females at ED6,

and phosphatidylcholine transporter activity (GO:0008525) at ED8 (Table S2b). In contrast, male samples at these time points showed fewer distinct functionalities and lower pathway diversity. These results suggest a more metabolically and structurally active CAM environment, favouring female embryos during early development, possibly reflecting differential developmental pacing or resource utilization. While early development reveals sex-biased pathways, several core functionalities are conserved across sexes. Shared enrichment of carbohydrate metabolic process (GO:0005975) and tricarboxylic acid cycle (GO:0006099) at all time points indicates a common energetic foundation required for CAM function, regardless of sex. The combined KEGG analysis of common proteins across sexes (Figure 4.4) revealed 25 enriched pathways, reinforcing the common roles of the CAM in both males and females. Upon closer examination of the male Kegg analysis (Figure 4.4), it was noted that there are fewer functional pathways, with ED10 and ED12 showing slightly fewer pathways. However, the number and complexity of functionalities were consistently greater in the female CAM proteome, especially in categories such as vesicle transport, lipid metabolism, and protein folding, suggesting a higher functional burden or regulatory flexibility. This is evident in Figure 4.4, where the abundance of identified proteins was consistently higher for female-based KEGG pathways compared to those of the male embryos. However, male-based KEGG analysis was more abundant at ED8, where the male CAM proteome was enriched compared to the female embryos. This study shows certain sex-specific protein differences; however, there are only minimal functional differences between males and females for the more common functionalities. Female CAM proteomes show slightly greater functional diversity (Table S2), with higher enrichment in protein-containing complexes, catalytic complexes, and cellular component organization shown in mostly all the KEGG pathways to be the most enriched, whereas male samples are more enriched for anion binding, small molecule

binding, and signalling (Figure 4.4), particularly at early stages (ED6–ED10), with differences diminishing by ED12. Understanding such sex-based molecular differences has implications not only for avian developmental biology but also for experimental design in embryology and poultry science, where sex-based variability should be considered in analyses and interventions. This enhances the utility of the CAM, paving the way for novel therapeutic strategies and diagnostic tools, paving biomedical innovations.

5. Conclusion

This study provides a comprehensive proteomic characterization of the CAM across early developmental timepoints (ED 6, 8, 10, and 12), with a novel focus on sex-linked protein expression. Using LC/MS/MS-based proteomics and functional bioinformatics analyses, we identified a total of 2,688 proteins with sex-specific expression patterns and protein constituents related to CAM functions, including gas exchange, calcium transport, immune defence, barrier protection, vessel formation, and embryonic blood elements. A significant finding is the sex-specific proteomic observed predominantly at earlier stages, with female CAM samples consistently exhibiting greater protein diversity and enriched pathways, especially related to autophagy, lipid transport, and protein folding. While many core CAM functions were conserved across sexes, these differences highlight sex as a biological variable that influences developmental trajectories even in extraembryonic tissues. Collectively, this research enhances our understanding of the CAM as a dynamic, multifunctional, and sex-responsive tissue, underscoring its potential not only as a model for developmental and biomedical research but also for non-invasive sex determination strategies in poultry science. These findings open new avenues for applications in early diagnostics and *in-ovo* interventions, offering a promising approach to reduce culling after

hatching of 1-day-old male chicks. This includes sex-specific developmental biology, positioning the CAM as a valuable platform for future innovation at the intersection of basic and applied life sciences.

6. Supporting Information (SI)

Supporting Information: Table S1. Total proteomic inventory for individual CAM samples (PDF). Table S2. DAVID analysis for timepoints ED 6-12 and combined for CAM tissue (PDF). Table S3. The emPAI values of the top hundred most abundant proteins identified in proteomics data of the CAM tissue samples at ED6-12 (PDF).

7. Acknowledgments

Funding for this study was provided by the Natural Sciences and Engineering Research Council (NSERC-Discovery; NSERC-Alliance), Egg Farmers of Canada (EFC), and Canadian Poultry Research Council (CPRC). During the preparation of this work, the authors utilized AI tools to enhance the language and readability of a specific component of the discussion. After using this tool/service, the authors reviewed and extensively edited the content as needed, taking full responsibility for the content of the publication.

CRediT: authorship contribution statement:

Sofhian Ali: Investigation, Methodology, Resources, Validation, Formal Analysis, Data Curation, Writing – _original draft, Writing – _review and editing. ***Tamer Ahmed:*** Project administration, Conceptualization, Methodology, Validation, Resources, Writing – _review and

editing, Funding acquisition. ***Maxwell Hincke:*** Supervision, Conceptualization, Methodology, Validation, Writing – _review and editing, Funding acquisition.

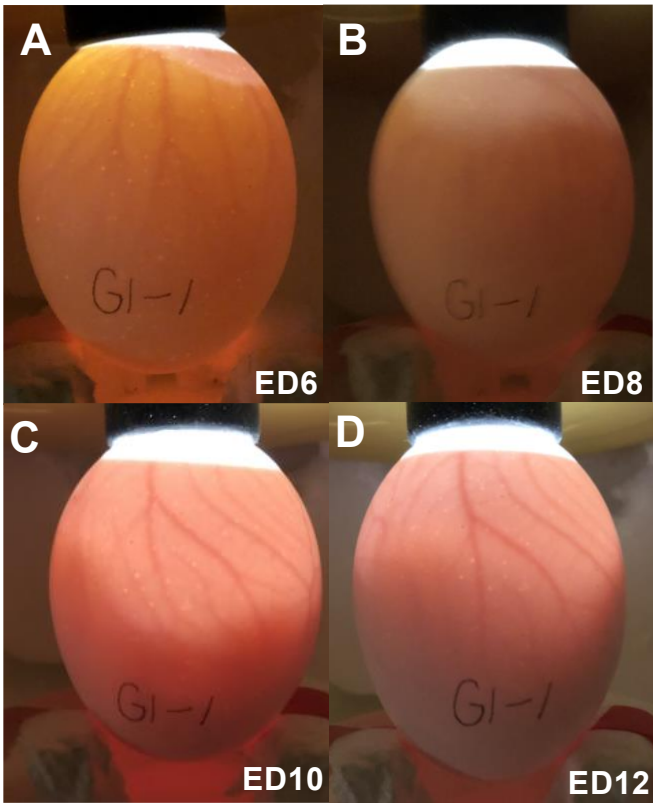

Figure 4.1. Fertilized White Leghorn egg shown under a high intensity Candler at A(ED6), B(ED8), C(ED10), and D(ED12) with a developing vascular system as the days pass, with a background yellow hue slowly turning red, reflecting the increased presence of blood vessels. Photographs courtesy of Sofhian Ali. Copyright 2025.

Table 4.1. Timing of chick embryo CAM development phases and associated critical events.

Embryonic development stage	Embryonic Event	Embryonic days (ED) 1 2 3 4 5 6 7 8 9 10 11 12 13 14 15 16 17 18 19 20 21
Establishment of germ layers	Development of the vascular system and immunity	
	Formation of extraembryonic tissues	
	Fusion of chorion and allantois begins	
	Evolution of chorioallantoic membrane (CAM)	
	Expansion of the CAM vasculature	
	Attachment of CAM to eggshell membrane	
	Initiation of sex determination	
Embryo completion	Complete CAM formation	
	Vascular network expansion	
	Gaseous exchange through CAM	
	Perfusion and full circulation through CAM	
	Immune barrier gene expression and protection	
	Calcium mobilization from eggshell	
	Intracellular calcium transport	
	The emergence of T and B immune cells	
Emergence	Peak CAM vasculature reaches maximum volume	
	Initiation of CAM degeneration	
	High-efficiency calcium uptake	
	Lung respiration begins (internal pipping)	
	Complete CAM regression/ hatched embryo	

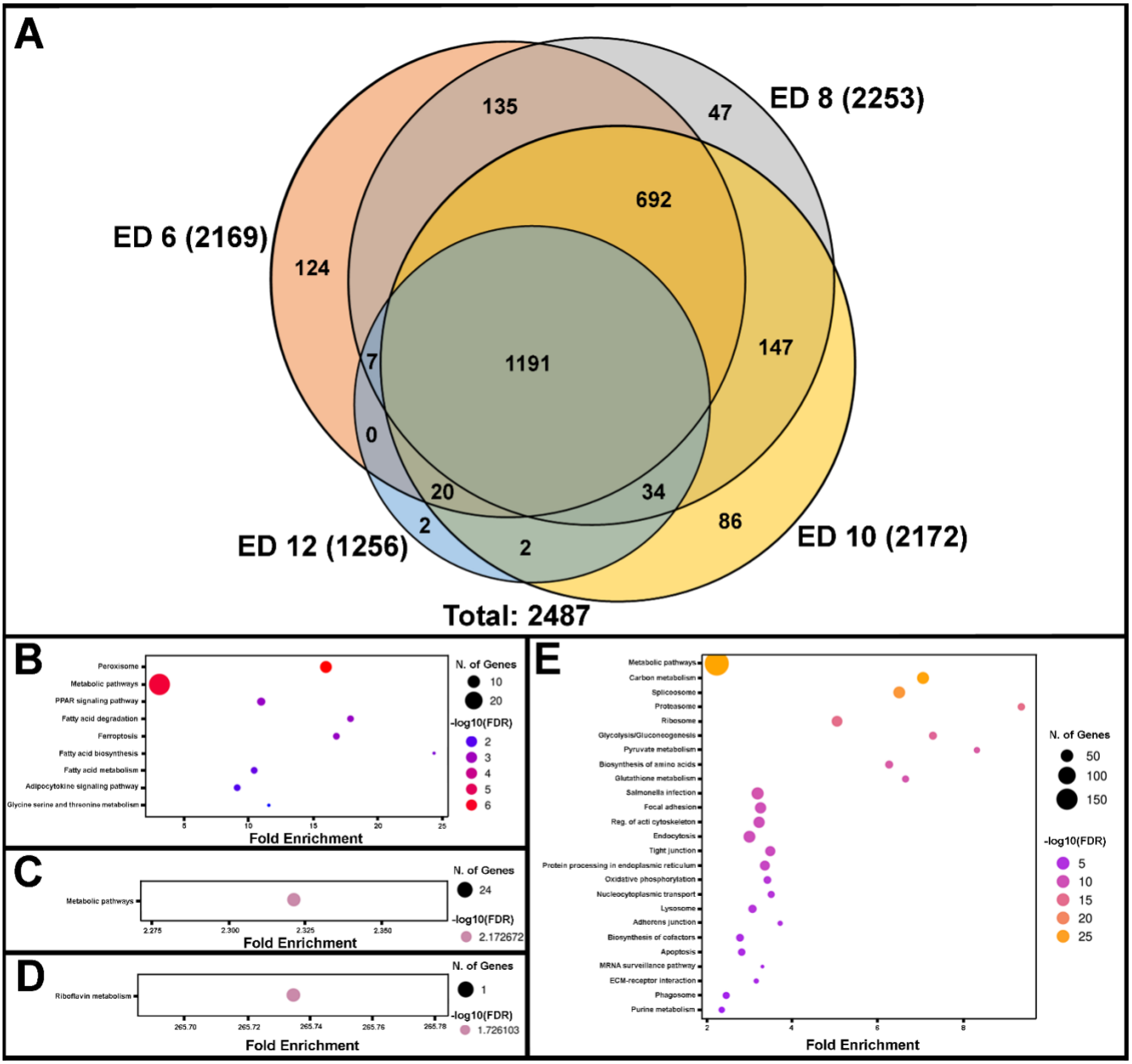

Figure 4.2. Compound Venn chart panel A displaying the distribution of identified common and unique CAM proteins for ED 6, ED8, ED10, ED12 and proteins identified in all four time points. Kegg pathway analysis, shown as a dot plot of clusters based on timepoints ED6 (B), ED10 (C), ED12 (D), and the combined clusters of ED6, 8, 10, and 12 (E), identifies clusters with P-values

<0.05. The size of the circles reflects the number of proteins in each pathway, and the colour gradient indicates the significance of the proteins within each pathway.

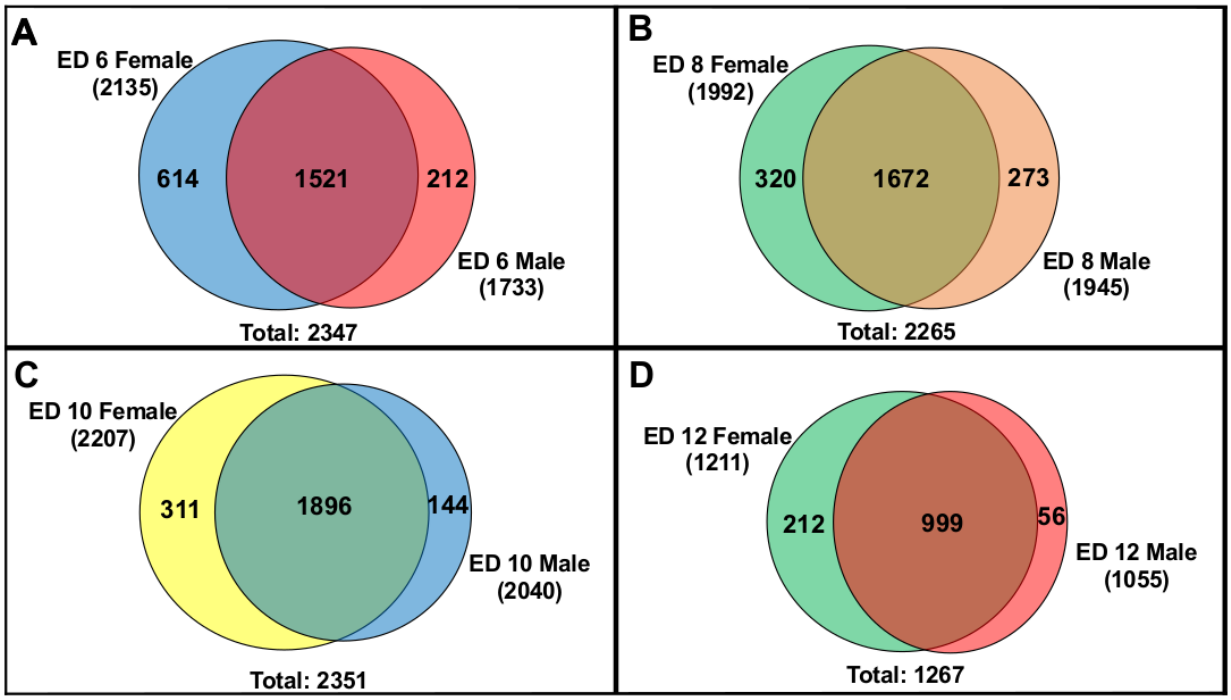

Figure 4.3. Venn chart displaying the distribution of numbers of identified common and unique CAM proteins between female and male samples during development. Panel A: ED 6, Panel B: ED8, Panel C: ED10 and Panel D: ED12.

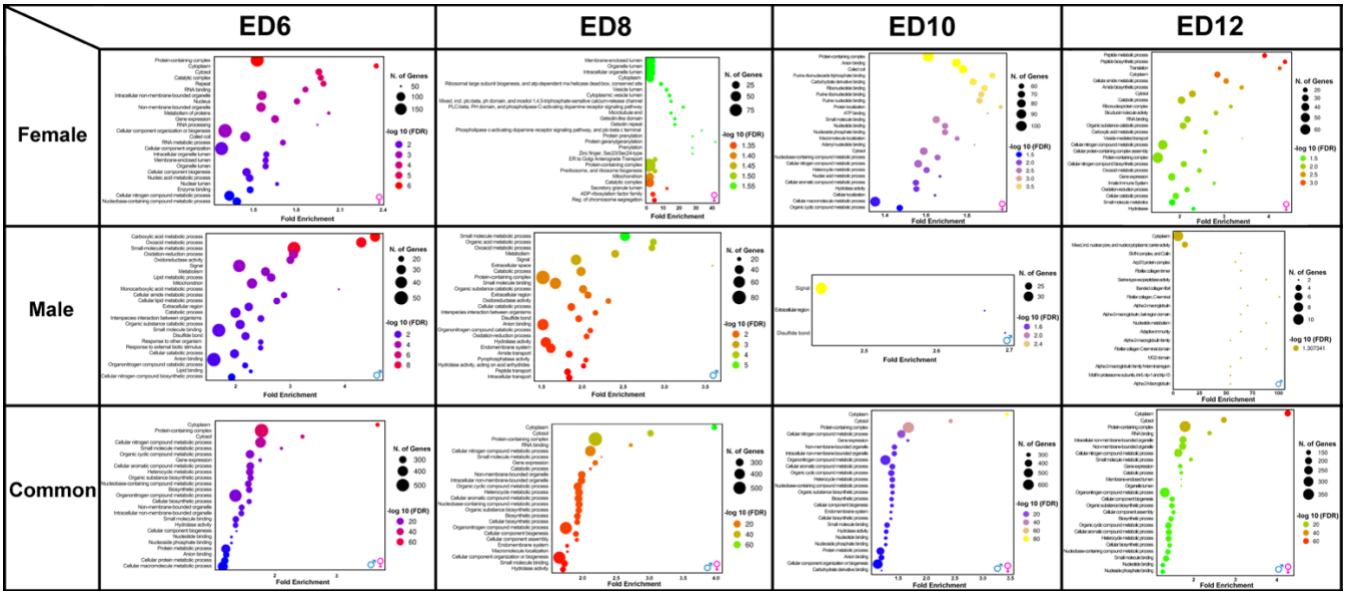

Figure 4.4. KEGG pathway analysis. Panel ED6, ED8, ED10 and ED12 as a dot plot. Each Kegg displays female, male, unique and common identified clustering functions with a P-value of <0.05. The size of the circles reflects the number of proteins in each pathway, and the color gradient indicates the significance of the highest *P* value (red) and the lowest *P* value (blue) for ED6, highest *P* value (green) and the lowest *P* value (orange) for ED8, the highest *P* value (yellow) and the lowest *P* value (blue) for ED10 and highest *P* value (red) and the lowest *P* value (green) for ED12.

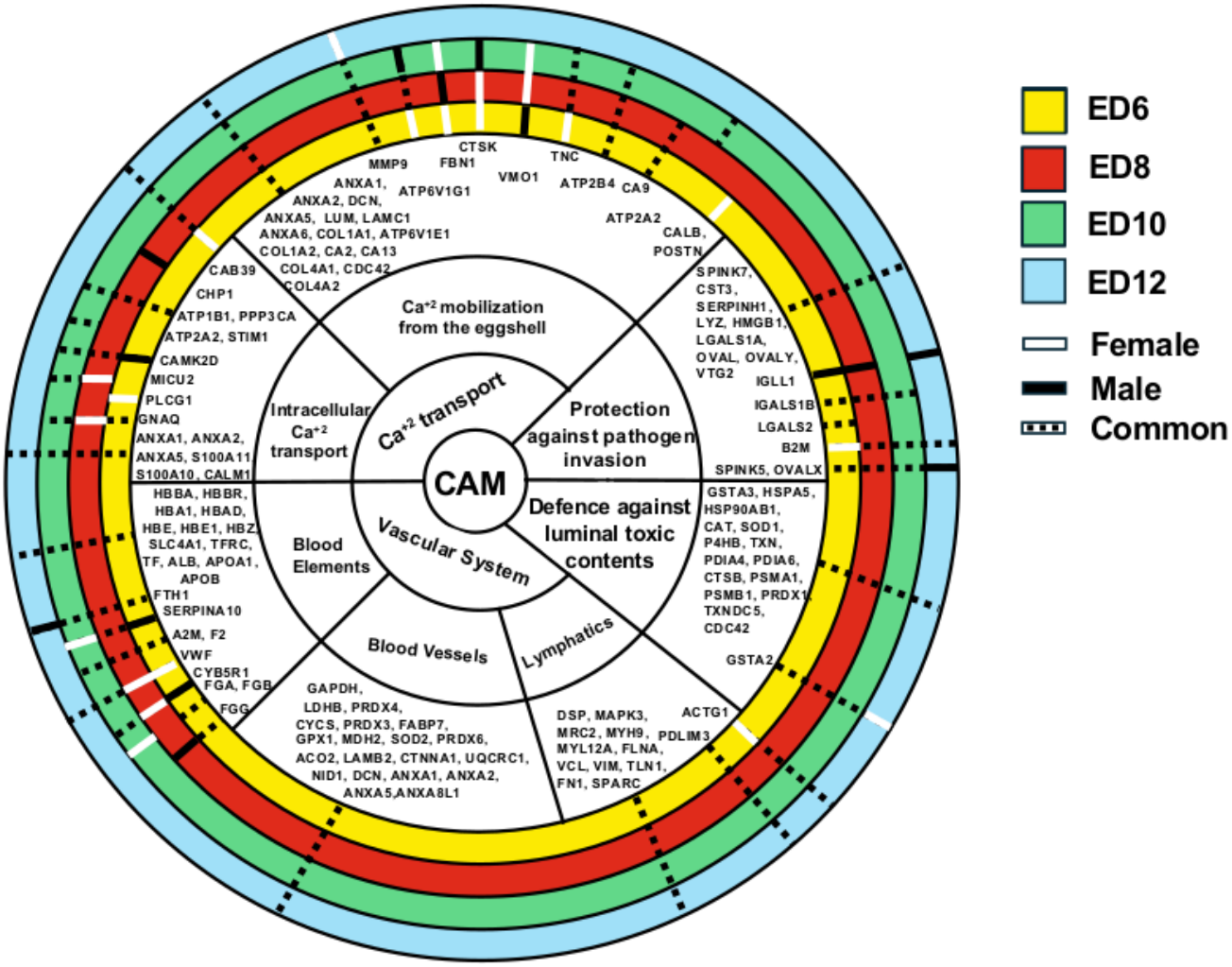

Figure 4.5. Mapping of CAM functionalities to proteomics results.

A CAM proteomic map highlighting CAM functionality: Ca^{2+} transport (Intracellular Ca2+ Transport and Ca2+ mobilization from the eggshell), the vascular system (blood elements, blood vessels, and lymphatics), and protection against pathogen invasion and luminal toxic contents, highlighted with their associated proteins. ED6 (yellow), ED8 (red), ED10 (green) and ED12 (blue) rings represent the different timepoints at which these proteins were identified, in male (black line) or female (white line) samples; proteins common to both sexes are represented with a dotted line. Proteins were selected using the following emPAI value thresholds: Blood vessels

(emPAI > 0.5), Lymphatics (emPAI > 0.1), defence against luminal toxic contents (emPAI > 0.5) and protection against pathogen invasion (emPAI > 0.2).

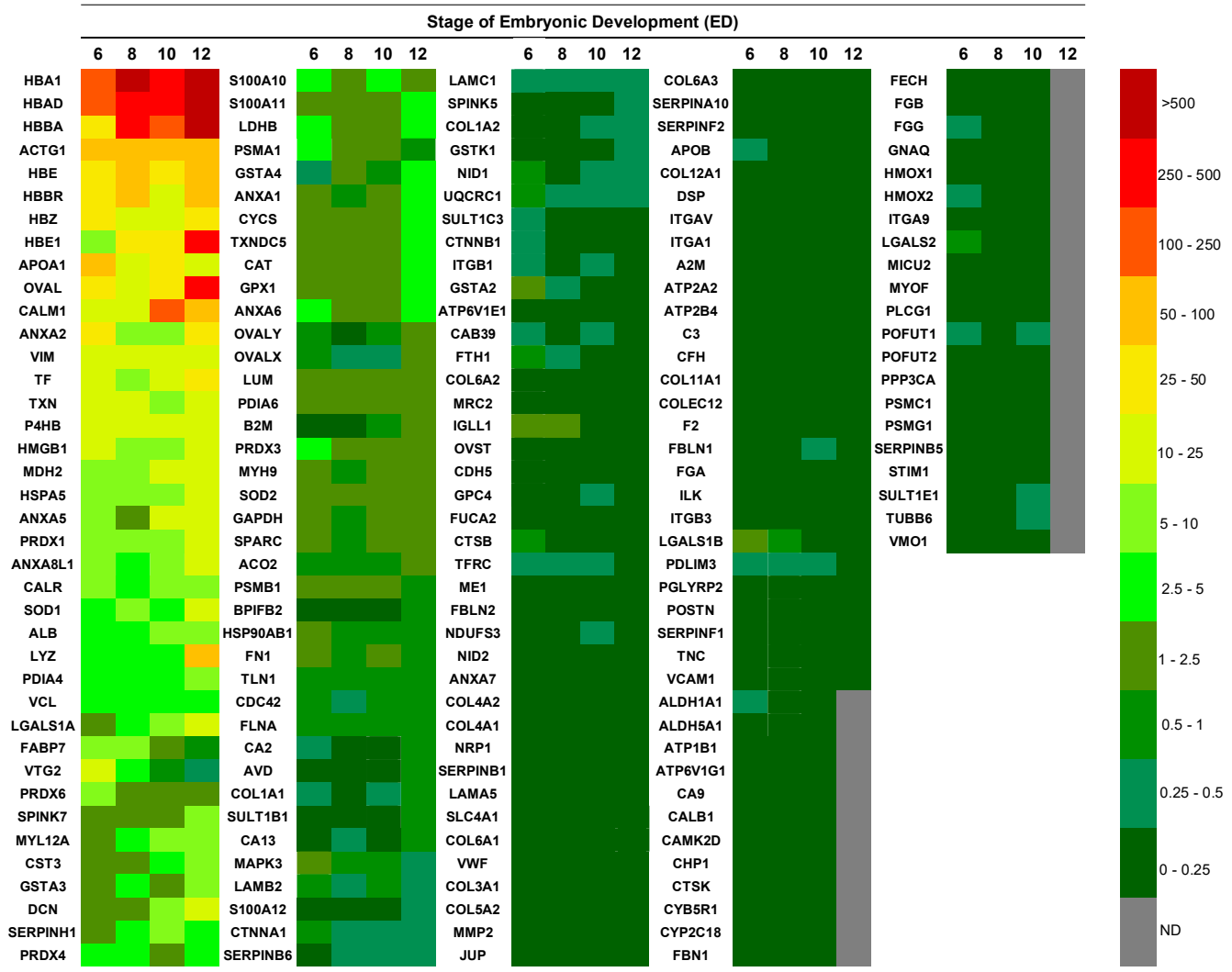

Figure 4.6. Heatmap of key CAM protein constituents playing critical roles in CAM development and embryonic growth. These proteins are grouped based on their abundance (emPAI values) across the developmental stages ED6, ED8, ED10, and ED12. The colour thresholds indicate emPAI abundance, from red (high abundance of 1018.60 emPAI highest cutoff threshold recorded) to green (low abundance). Proteins not detected (ND) are assigned grey.

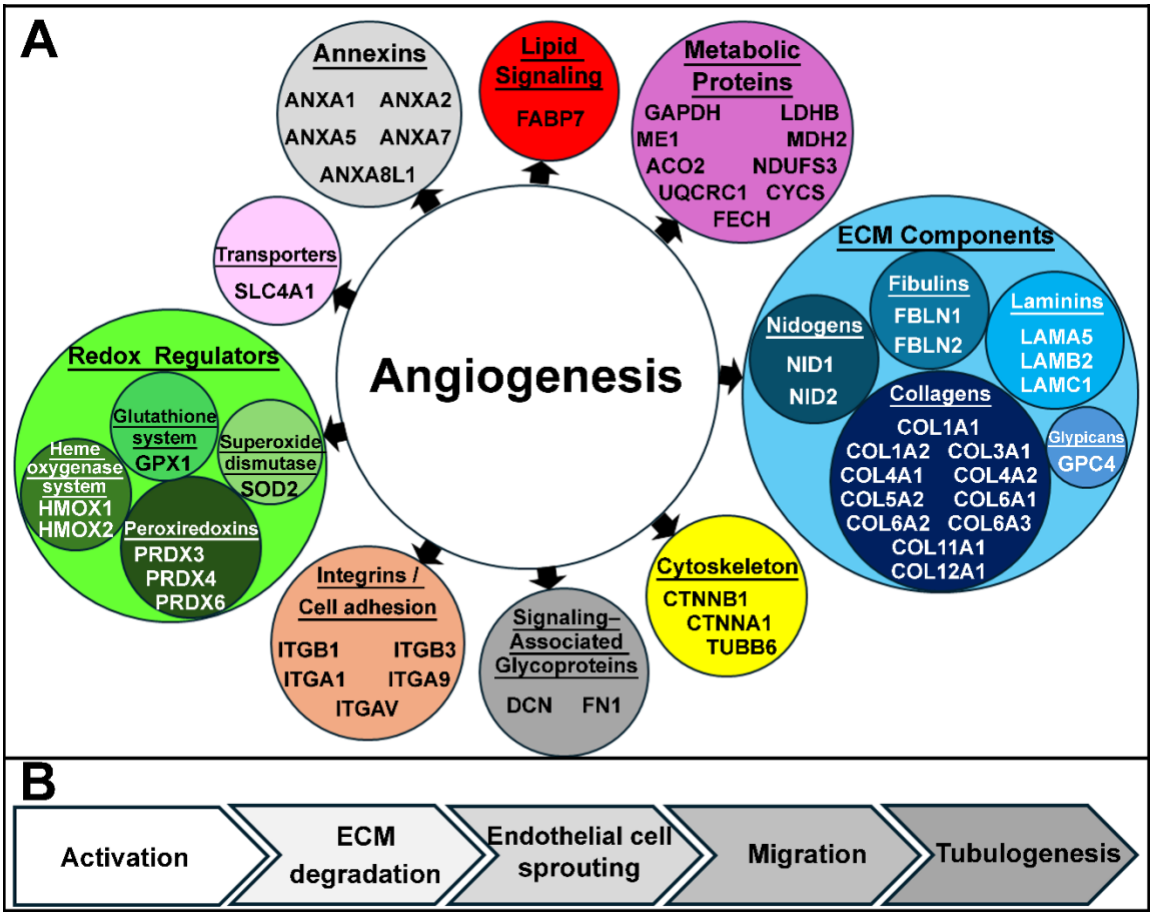

Figure 4.7. Functional categorization of 52 chicken proteins associated with angiogenesis.

A). The upper panel groups proteins into major functional categories, including ECM components, integrins, annexins, redox regulators, signalling-associated glycoproteins, and transporters, as well as metabolic, cytoskeletal, and lipid-signalling proteins. These groups illustrate how structural, metabolic, and regulatory factors coordinate / reflect the progression of CAM angiogenesis. B). The lower panel outlines the key angiogenic stages: endothelial activation, ECM degradation, sprouting, migration, and tube (lumen) formation.

Table 4.2. Summary of protein family clusters identified at all timepoints of CAM development (ED6, 8, 10 and 12).

No.	Protein family name	Family members identified in CAM
1	Collagens	*COL1A1, COL1A2, COL2A1, COL3A1, COL4A1, COL4A2, COL4A5, COL5A1, COL5A2, COL6A1, COL6A2, COL6A3, COL11A1, COL12A1, COL14A1*
2	Translation initiation factor	*DENR, EIF1AX, EIF2S1, EIF2S2, EIF2S3, EIF2A, EIF3A, EIF3B, EIF3E, EIF3F, EIF3H, EIF3I, EIF3J, EIF3K, EIF3L, EIF3M, EIF3G, EIF4G1, EIF4G2, EIF4G3, EIF4A2, EIF4E, EIF5, EIF5A2, EIF5B, EIF6*
3	DEAD-box helicase	*DDX1, DDX17, DDX19, DDX3X, DDX42, DDX46, DDX5, DDX6*
4	Heat shock protein	*DNAJA2, DNAJB1, DNAJB11, DNAJC1, DNAJC10, DNAJC3, DNAJC7, DNAJC8, DNAJC9, HSPA5, HSBP1, HSP90AB1, HSP90B1, HSPA14, HSPA2, HSPA4, HSPA4L, HSPA8, HSPA9, HSPB1, HSPD1, HSPE1, HSPH1*
5	Motor proteins	*DNAAF10, DYNC1H1, DYNC1I2, DYNC1LI1, DYNC1LI2, DYL1, DYNLRB1, DYNLT1, KIF13B, KIF15, KIF16B, KIF26B, KIF5B, KIF7*
6	Integrins	*ILK, ITGA1, ITGA4, ITGA9, ITGAV, ITGB1, ITGB3*
7	Cadherins	*CDH1, CDH2, CDH3, CDH5, CDH6, CDH11, CDH13, CDH17*
8	Heterogenous nuclear ribonucleoprotein	*HNRNPAB, HNRNPA0, HNRNPA1, HNRNPA2B1, HNRNPA3, HNRNPD, HNRNPDL, HNRNPH1, HNRNPH3, HNRNPKL, HNRNPLL, LOC101749377, HNRNPM, HNRNPR, HNRNPU, HNRNPUL1*
9	Laminin protein	*LAMA2, LAMA4, LAMA5, LAMB4, LAMC1, LAMB2*
10	Insulin growth factor	*IGF1R, IGF2BP1, IGF2BP3, IGF2R, IGFBP2, IGFBP7*
11	Zinc finger protein	*ZC3HC1, ZC3H11A, ZC3H15, ZC3H18, ZNF207, ZNF326, ZRANB2, LOC427010, ZPR1*
12	Transport channels Na+/K+-ATPase and H+	*ATP6V1A, ATP6V1B2, ATP6V1C1, ATP6V1E1, ATP6V1G1, ATP6V1H, ATP1A1, ATP1B1*
13	Histones	*H-10, H1-01, H1-10, H1-1R, H2AC39, H2A2BL, H2AZ1, H2BC32, H3-3A, H4C37, H4C38*
14	Carbonic anhydrase	*CA2, CA8, CA9, CA13*
15	Annexin	*ANXA1, ANXA2, ANXA4, ANXA5, ANXA6, ANXA7, ANXA8L1, ANXA11*
16	Serpin	*SPIA4, SPIA1, SPIA5, SERPINA10, SERPINB1, SERPINB5, SERPINC1, SERPIND1, SERPINF1, SERPINF2, SERPING1, SERPINH1, SERPINI1, SERPINB6*
17	Peroxiredoxin	*PRDX1, PRDX3, PRDX4, PRDX6*
18	charged multivesicular body protein	*CHMP2A, CHMP4B, CHMP5, CHMP6, CHMP7*
19	Cellular death proteins	*CASP1, CASP3, CASP6, CASP7, CASP8, CASP9, CTSA, CTSB, CTSC, CTSD, CTSH, CTSK, CTSS, CTSV, CTSZ*
20	Tubulin	*TUBA1A, LOC100857858, TUBB1, TUBB2B, TUBB4B, TUBB6, TUBB, TUB5A*

Chapter 5: General Discussion and Conclusions

The intensifying global demand for ethically compliant, high-quality poultry products has prompted a critical re-evaluation of avian hatchery management practices, particularly the culling of 1-day-old male chicks in commercial layer lines. Although operationally indispensable for preserving economic efficiency under current production approaches, this intervention elicits profound ethical, ecological, and developmental concerns (Gautron et al., 2021). Consequently, international initiatives emphasize sustainable, embryologically informed alternatives (de Haas et al., 2021). This thesis aims to provide tools to circumvent the culling of 1-day-old male chicks in the layer industry. To address this, a novel proteomics-based approach to sex determination in developing chicken embryos was explored using the CAM.

One of the core parts of the working hypotheses, associated with objective 1, is that embryonic viability, growth, and development will be unaffected or only slightly affected by sampling a minute quantity of CAM for immune interrogation. A significant portion of the project effort has been devoted to CAM manipulation experiments. The goal of these experiments was to evaluate and optimize the use of eggshell (ES) disinfection, ES drilling, surgical equipment, needles, and sealant to preserve embryo viability. Further optimization will be necessary to refine these techniques. Moreover, the results indicate that the CAM at ED 6 is more challenging to sample, with reduced embryo viability (as assessed at ED 16) due to its greater delicacy compared to ED 8 and 10. Harvesting CAM at ED 8 and 10 is more compatible with embryo viability than at ED 6, when the CAM is more vulnerable, likely because the CAM and the embryo itself have further developed on those days and are less sensitive to manipulation and stress. Traditional Ethanol (70%) was assessed to disinfect eggs in the study. Benzalkonium chloride (0.13%) or Dettol (0.6%)

was found to be a better alternative, as the study showed that embryonic viability was preserved when it was used as an alternative to ethanol. Additionally, the hole size drilled in the ES to access the CAM was optimized and found to be crucial. The hole sizes explored (0.8mm, 1.5 mm, 2.5 mm, and 3 mm) were obtained using different Dremel rotary bits, which exposed the interior of the egg. ESM removal often reduced survival, and sampling at inappropriate locations or early stages led to high mortality. We also focused on the sampling strategy to remove minute amounts of CAM using various surgical manipulations, including suction force (with a pen-shaped tool) and using a micropipette/tip to latch on and harvest a fragment of CAM. Manipulations at ED8 and ED10 generally maintained higher viability and weights than ED6, especially when using minimally invasive micropipette suction for CAM sampling. Moreover, alternative sampling methods, such as micropipette suction, may offer a less invasive and more effective means of collecting CAM samples. The use of liquid sealants shows potential for preserving embryo health, with silicone sealant being the most effective throughout the study. This study highlighted critical aspects of early CAM manipulation (days 6, 8, and 10 of development) and their impact on embryo survival, finding that further optimization is desirable. Overall, these results contribute to a better understanding of the challenges involved in developing innovative CAM assessment techniques that maintain embryo viability, a crucial requirement for pre-hatch embryo sexing based on CAM analysis.

Comprehensive proteomic interrogation of chorioallantoic membrane (CAM) samples harvested at embryonic days 6, 8, 10, and 12 was performed to delineate sex-specific protein signatures as well as attribute important multifunctionality of the CAM with respect to various development phases of the embryonic life. The outcomes substantiate the premise that the CAM, owing to its

vascular integration, accessibility, and indispensable physiological functions, constitutes a feasible biomaterial interface for early, non-invasive embryo sex determination. Upon validation, these molecular entities demonstrate potential as biomarkers for early identification of female embryos before nociceptive onset, thereby addressing ethical imperatives (Kollmansperger et al., 2023). Our study, based on project objectives 2a (identifying W-encoded proteins on the CAM during early embryonic development using proteomics and bioinformatics) and 2b (using qPCR to validate proteomics-based sex prediction for W-specific genes), generated two proteomics datasets. These two datasets were combined, enabling the identification of a total of 2,688 proteins in CAM tissue samples, with 2,347, 2,265, 2,351, and 1,267 proteins detected at ED 6, 8, 10, and 12, respectively. Notably, 1,191 common proteins were identified across all stages, while 124, 47, 86, and 2 proteins were uniquely expressed at ED 6, 8, 10, and 12, respectively. Notably, a sex-specific analysis identified 614, 320, 314, and 212 proteins that were uniquely expressed in female embryos, and 212, 273, 144, and 56 proteins only in male embryos at ED 6, 8, 10, and 12, respectively. A number of W-encoded proteins were also identified, which were then analyzed further through bioinformatics to move forward with the next stage of the project, the production of antibodies to synthetic peptides, which is currently ongoing. Due to confidentiality concerns with respect to premature disclosure of intellectual property, the names and identifiers of certain W-encoded proteins and their Z-encoded homologs have been omitted from the thesis.

In addition to sex identification, this research yielded valuable insights into the functional complexity of the CAM throughout development, which is highlighted in Chapter 4 of the thesis. Distinct proteomic profiles associated with various functions, including calcium mobilization, immune defence, blood and vascular development, and intracellular transport, were mapped across

different developmental time points and between sexes. These patterns reflect the multifunctional nature of the CAM (Nowak-Sliwinska et al., 2014) and variations in gene expression within the CAM. Notably, several protein families identified here, annexins, collagens, integrins, serpins, and globins, overlap with previous CAM datasets and other embryonic tissues, suggesting conserved roles in angiogenesis, extracellular matrix remodelling, and immune defence (Soulet et al., 2013; Nowak-Sliwinska et al., 2014; Ahmed et al., 2019; Ahmed et al., 2022). At the same time, the high-resolution proteomic mapping in this work highlights developmental stage-specific shifts in protein abundance, particularly among hemoglobins, metabolic enzymes, and redox regulators, providing molecular depth beyond prior descriptive studies. These findings position the CAM as a sex-responsive tissue, raising important questions about the role of sex as a biological variable in avian embryology. They also carry practical implications: the ability to detect sex-linked proteomic signatures in extraembryonic tissues opens the door to novel *in-ovo* sexing approaches.

The application of proteomic analyses for *in-ovo* sex determination presents both experimental opportunities and developmental constraints. While current sexing strategies primarily rely on imaging, endocrine profiling, or genomic interrogation, proteomic approaches could offer a complementary or potentially superior mechanism. Protein-based detection may enable earlier, high-fidelity sex specification, particularly upon the identification of robust W–chromosome–linked embryonic biomarkers. However, further work is required to develop fast, cost-effective, and minimally invasive methods for detecting these proteins at scale, including immunoassays or biosensor technologies that can operate in industrial hatchery settings. The results presented in Chapter 4 demonstrate that the chick CAM is not only a model of vascular biology and barrier defence but also a sex-responsive tissue with proteomic features reflecting developmental

complexity. By profiling the CAM proteome across ED6-12 and identifying sex-specific protein expression, new molecular insights into its role in embryonic development are gained, as well as open pathways toward applied innovations for *in-ovo* diagnostics. These findings reinforce the CAM's value as both a basic research model and a platform for translational applications at the interface of developmental biology, biomedical science, and poultry production.

This thesis demonstrates the feasibility of using the CAM as a target for early, *in-ovo* sex identification through proteomic analysis. If challenges to preserving embryo viability can be overcome, it will be a key cornerstone of the project. By identifying proteins differentially expressed between male and female embryos at key developmental time points, this study lays the groundwork for developing a novel, humane method to prevent the culling of male chicks. Such an approach aligns with the growing ethical demands of consumers and regulatory bodies, offering the potential to improve sustainability and efficiency in the global poultry industry. Beyond the immediate application of sexing, this research also enriches our understanding of CAM biology, avian development, and the broader implications of proteomic technologies in agricultural science. The integration of this knowledge with existing and emerging sexing technologies prioritizes both productivity and animal welfare.

Future work should focus on validating the candidate protein biomarkers identified. In these ongoing experiments, we have raised sensitive and specific polyclonal antibodies against synthetic peptides corresponding to relatively unique sequences within W-encoded protein(s). The most suitable W-encoded sequences for synthetic peptide synthesis were identified, followed by the coupling of these peptides to KLH and the raising of polyclonal antibodies in rabbits. Several W-

encoded proteins were evaluated. In each case, the affinity-purified antibodies were cross-absorbed using a synthetic peptide sequence based on a similar region of the Z-encoded homologues. The titer and specificity of affinity-purified antibodies were verified by ELISA conducted by our industrial partner (Genscript Biotech Inc.), and ongoing trials using in-house CAM immunohistochemistry are underway (UOttawa). Future directions for this project will also include optimizing the immunoassay for one or more candidate W-chromosome-linked proteins in CAM tissue. Results from Western blotting (WB) and immunohistochemistry will be evaluated using CAM tissue from male and female embryos. This project may lead to the development of an immunoassay, possibly an enzyme-linked immunosorbent assay (ELISA), to quickly, sensitively, and precisely detect a sex-specific W-encoded protein, enabling *in-ovo* sex prediction.

References

Acsa, I., Lilly Caroline, B., Philip Njeru, N., & Lucy Wanjiru, N. (2021). Preliminary study on disinfectant susceptibility/resistance profiles of bacteria isolated from slaughtered village free-range chickens in nairobi, kenya. International Journal of Microbiology, 2021, 1–7. https://doi.org/10.1155/2021/8877675

Ahmed, T. A. E., Kulshreshtha, G., Younes, M., & Hincke, M. T. (2023). Eggshell and Membranes. In *Handbook of Egg Science and Technology* (pp. 51–72). CRC Press.

Ahmed, T. A. E., Suso, H.-P., & Hincke, M. T. (2017). In-depth comparative analysis of the chicken eggshell membrane proteome. Journal of Proteomics, 155, 49–62. https://doi.org/10.1016/j.jprot.2017.01.002

Ahmed, T. A. E., Suso, H.-P., Maqbool, A., & Hincke, M. T. (2019). Processed eggshell membrane powder: Bioinspiration for an innovative wound healing product. Materials Science and Engineering: C, 95, 192–203. https://doi.org/10.1016/j.msec.2018.10.054

Ahmed, T. A., Cordeiro, C. M., Elebute, O., & Hincke, M. T. (2022). Proteomic analysis of chicken chorioallantoic membrane (CAM) during embryonic development provides functional insight. *BioMed Research International*, *2022*, 1–17. https://doi.org/10.1155/2022/7813921

Ali Laghari, Z. (2015). Effects of a single dose of ethanol on survival rate and angiogenesis of chick embryo. Animal and Veterinary Sciences, 3(1), 8. https://doi.org/10.11648/j.avs.20150301.12

Anderson, R. E., Gay, C. V., & Schraer, H. (1981). Ultrastructural localization of carbonic anhydrase in the chorioallantoic membrane by immunocytochemistry. Journal of

Histochemistry & Cytochemistry, 29(10), 1121–1127. https://doi.org/10.1177/29.10.6170666

Baker, B. I., Torrey, S., Widowski, T. M., Turner, P. V., Knezacek, T. D., Nicholds, J., Crowe, T. G., & Schwean-Lardner, K. (2019). Evaluation of carbon dioxide induction methods for the euthanasia of day-old cull broiler chicks. Poultry Science, 98(5), 2043–2053. https://doi.org/10.3382/ps/pey581

Bellott, D. W., Skaletsky, H., Cho, T.-J., Brown, L., Locke, D., Chen, N., Galkina, S., Pyntikova, T., Koutseva, N., Graves, T., Kremitzki, C., Warren, W. C., Clark, A. G., Gaginskaya, E., Wilson, R. K., & Page, D. C. (2017). Avian w and mammalian Y chromosomes convergently retained dosage-sensitive regulators. *Nature Genetics*, *49*(3), 387–394. https://doi.org/10.1038/ng.3778

Bonnefous, C., Collin, A., Guilloteau, L. A., Guesdon, V., Filliat, C., Réhault-Godbert, S., Rodenburg, T. B., Tuyttens, F. A. M., Warin, L., Steenfeldt, S., Baldinger, L., Re, M., Ponzio, R., Zuliani, A., Venezia, P., Väre, M., Parrott, P., Walley, K., Niemi, J. K., & Leterrier, C. (2022). Welfare issues and potential solutions for laying hens in free range and organic production systems: A review based on literature and interviews. Frontiers in Veterinary Science, 9. https://doi.org/10.3389/fvets.2022.952922

Brekken, R. A., & Sage, E. H. (2000). SPARC, a matricellular protein: At the crossroads of cell–matrix. Matrix Biology, 19(7), 569–580. https://doi.org/10.1016/S0945-053X(00)00105-0

Castro, F. L. S., Chai, L., Arango, J., Owens, C. M., Smith, P. A., Reichelt, S., DuBois, C., & Menconi, A. (2023). Poultry industry paradigms: Connecting the dots. Journal of Applied Poultry Research, 32(1), 100310. https://doi.org/10.1016/j.japr.2022.100310

Caunt, M., Huang, Y.-Q., Brooks, P. C., & Karpatkin, S. (2003). Thrombin induces neoangiogenesis in the chick chorioallantoic membrane. Journal of Thrombosis and Haemostasis, 1(10), 2097–2102. https://doi.org/10.1046/j.1538-7836.2003.00426.x

Chen, L., Wang, S., Feng, Y., Zhang, J., Du, Y., Zhang, J., Ongeval, C. V., Ni, Y., & Li, Y. (2021). Utilisation of chick embryo chorioallantoic membrane as a model platform for imaging-navigated biomedical research. *Cells*, *10*(2), 463. https://doi.org/10.3390/cells10020463

Ching, C. T. S., Wang, C.-K., Tang, P.-C., Ha, M.-K., Li, C., Chiu, H.-N., Yao, F. Y.-D., Nhan, N. C., Hieu, N. V., & Phan, T.-L. (2023). Bioimpedance-measurement-based non-invasive method for in ovo chicken egg sexing. *Biosensors*, *13*(4), 440. https://doi.org/10.3390/bios13040440

Chu, P.-Y., Koh, A. P.-F., Antony, J., & Huang, R. Y.-J. (2022). Applications of the chick chorioallantoic membrane as an alternative model for cancer studies. Cells Tissues Organs, 211(2), 222–237. https://doi.org/10.1159/000513039

Clark, E. R., & Clark, E. L. (1919). *On the origin and early development of the lymphatic system of the chick*. Carnegie Institution of Washington.

Cook, M. I., & Monaghan, P. (2004). Sex differences in embryo development periods and effects on avian hatching patterns. Behavioral Ecology, 15(2), 205–209. https://doi.org/10.1093/beheco/arg096

Cordeiro, C. M. M., & Hincke, M. T. (2016). Quantitative proteomics analysis of eggshell membrane proteins during chick embryonic development. *Journal of Proteomics*, *130*, 11–25. https://doi.org/10.1016/j.jprot.2015.0.014

Corion, M., Santos, S., De Ketelaere, B., Spasic, D., Hertog, M., & Lammertyn, J. (2023). Trends in in ovo sexing technologies: Insights and interpretation from papers and patents. *Journal*

of Animal Science and Biotechnology, *14*(1), 102. https://doi.org/10.1186/s40104-023-00898-1

Da Silva, M., Beauclercq, S., Harichaux, G., Labas, V., Guyot, N., Gautron, J., Nys, Y., & Rehault-Godbert, S. (2015). The family secrets of avian egg-specific ovalbumin and its related proteins y and x. Biology of Reproduction, 93(3). https://doi.org/10.1095/biolreprod.115.130856

Dakhel, S., Davies, W. I. L., Joseph, J. V., Tomar, T., Remeseiro, S., & Gunhaga, L. (2021). Chick fetal organ spheroids as a model to study development and disease. BMC Molecular and Cell Biology, 22(1), 37. https://doi.org/10.1186/s12860-021-00374-6

de Haas, E. N., Oliemans, E., & van Gerwen, M. A. A. M. (2021). The need for an alternative to culling day-old male layer chicks: A survey on awareness, alternatives, and the willingness to pay for alternatives in a selected population of dutch citizens. *Frontiers in Veterinary Science*, *8*. https://doi.org/10.3389/fvets.2021.662197

DeRuiter, C., & Doty, M. (2011, June 21). *Gastrulation in Gallus gallus (domestic chicken)*. Embryo Project Encyclopedia. Retrieved August 28, 2025, from https://embryo.asu.edu/pages/gastrulation-gallus-gallus-domestic-chicken

Deryugina, E. I., & Quigley, J. P. (2008). Chick embryo chorioallantoic membrane model systems to study and visualize human tumor cell metastasis. Histochemistry and Cell Biology, 130(6), 1119–1130. https://doi.org/10.1007/s00418-008-0536-2

Di Concetto, A., Morice, O., Corion, M., & Santos, S. (2023, January 11). White Paper – Chick and Duckling Killing: Achieving an EU-Wide Prohibition. European Institute for Animal Law & Policy.

Dombre, C., Guyot, N., Moreau, T., Monget, P., Da Silva, M., Gautron, J., & Réhault-Godbert, S. (2017). Egg serpins: The chicken and/or the egg dilemma. Seminars in Cell & Developmental Biology, 62, 120–132. https://doi.org/10.1016/j.semcdb.2016.08.019

Eliceiri, B. P., & Cheresh, D. A. (1998). The role of αv integrins during angiogenesis. Molecular Medicine, 4(12), 741–750. https://doi.org/10.1007/BF03401768

Eliceiri, B. P., & Cheresh, D. A. (1999). The role of αv integrins during angiogenesis: Insights into potential mechanisms of action and clinical development. Journal of Clinical Investigation, 103(9), 1227–1230. https://doi.org/10.1172/JCI6869

Epp, M. (2016, December 19). Hypereye: A game changer – Canadian Poultry Magazine. https://www.canadianpoultrymag.com/hypereye-a-game-changer-30033/

Gabrielli, M. G., & Accili, D. (2010). The Chick Chorioallantoic Membrane: A model of molecular, structural, and functional adaptation to transepithelial ion transport and barrier function during embryonic development. *Journal of Biomedicine and Biotechnology*, *2010*, 1–12. https://doi.org/10.1155/2010/940741

Gabrielli, M. G., Materazzi, G., Cox, J. V., & Menghi, G. (2001). Specialised cell types in the chorioallantoic membrane express carbonic anhydrase during chick embryogenesis. Journal of Anatomy, 198(Pt 2), 229–238. https://doi.org/10.1046/j.1469-7580.2001.19820229.x

Gautron, J., Réhault-Godbert, S., Van De Braak, T. G. H., & Dunn, I. C. (2021). Review: What are the challenges facing the table egg industry in the next decades and what can be done to address them? Animal, 15, 100282. https://doi.org/10.1016/j.animal.2021.100282

Göhler, D., Fischer, B., & Meissner, S. (2017). In-ovo sexing of 14-day-old chicken embryos by pattern analysis in hyperspectral images (VIS/NIR spectra): A non-destructive method for

layer lines with gender-specific down feather color. *Poultry Science*, *96*(1), 1–4. https://doi.org/10.3382/ps/pew282

Government of Canada, S. C. (2025, May 29). *The Daily—Poultry and egg statistics, May 2025 and annual 2024*. https://www150.statcan.gc.ca/n1/daily-quotidien/250529/dq250529c-eng.htm

Gurtner, G. C., Davis, V., Li, H., McCoy, M. J., Sharpe, A., & Cybulsky, M. I. (1995). Targeted disruption of the murine VCAM1 gene: Essential role of VCAM-1 in chorioallantoic fusion and placentation. Genes & Development, 9(1), 1–14. https://doi.org/10.1101/gad.9.1.1

Habashy, W. S., Milfort, M. C., Rekaya, R., & Aggrey, S. E. (2021). Molecular and cellular responses of DNA methylation and thioredoxin system to heat stress in meat-type chickens. Animals, 11(7), 1957. https://doi.org/10.3390/ani11071957

Halgrain, M., Bernardet, N., Crepeau, M., Même, N., Narcy, A., Hincke, M., & Réhault-Godbert, S. (2022). Eggshell decalcification and skeletal mineralization during chicken embryonic development: Defining candidate genes in the chorioallantoic membrane. Poultry Science, 101(2), 101622. https://doi.org/10.1016/j.psj.2021.101622

Hamburger, V., & Hamilton, H. L. (1951). A series of normal stages in the development of the chick embryo. Journal of Morphology, 88(1), 49–92. https://doi.org/10.1002/jmor.1050880104

Hamburger, V., & Hamilton, H. L. (1992). A series of normal stages in the development of the chick embryo. Developmental Dynamics, 195(4), 231–272. https://doi.org/10.1002/aja.1001950404

He, L., Martins, P., Huguenin, J., Van, T.-N.-N., Manso, T., Galindo, T., Gregoire, F., Catherinot, L., Molina, F., & Espeut, J. (2019). Simple, sensitive and robust chicken specific sexing

assays, compliant with large scale analysis. *PLOS ONE*, *14*(3). https://doi.org/10.1371/journal.pone.0213033

Hendrix Genetics. (2023, May 24). Orbem: Revealing what's hidden inside the hatching egg. Laying Hens. Retrieved August 28, 2025, from https://layinghens.hendrix-genetics.com/en/articles/orbem-revealing-whats-hidden-inside-the-hatching-egg/

Hennequet-Antier, C., Halgrain, M., & Réhault-Godbert, S. (2024). RNA-seq dataset of the chorioallantoic membrane of male and female chicken embryos, after 11 and 15 days of incubation. Data in Brief, 56, 110830. https://doi.org/10.1016/j.dib.2024.110830

Hincke, M. T., Da Silva, M., Guyot, N., Gautron, J., McKee, M. D., Guabiraba-Brito, R., & Réhault-Godbert, S. (2019). Dynamics of structural barriers and innate immune components during incubation of the avian egg: Critical interplay between autonomous embryonic development and maternal anticipation. Journal of Innate Immunity, 11(2), 111–124. https://doi.org/10.1159/000493719

Horrocks, N. P., Hine, K., Hegemann, A., Ndithia, H. K., Shobrak, M., Ostrowski, S., Williams, J. B., Matson, K. D., & Tieleman, B. I. (2014). Are antimicrobial defences in bird eggs related to climatic conditions associated with risk of trans-shell microbial infection? Frontiers in Zoology, 11(1), 49. https://doi.org/10.1186/1742-9994-11-49

Kollmansperger, S., Anders, M., Werner, J., Saller, A. M., Weiss, L., Süß, S. C., Reiser, J., Schneider, G., Schusser, B., Baumgartner, C., & Fenzl, T. (2023). Nociception in chicken embryos, part ii: Embryonal development of electroencephalic neuronal activity in ovo as a prerequisite for nociception. *Animals*, *13*(18), 2839. https://doi.org/10.3390/ani13182839

Kummer, M. (2023, December 6). Pros and cons of raising leghorns for eggs. *Kummer Homestead*. https://kummerhomestead.com/raising-leghorns-for-eggs/

Kunz, P., Schenker, A., Sähr, H., Lehner, B., & Fellenberg, J. (2019). Optimization of the chicken chorioallantoic membrane assay as reliable in vivo model for the analysis of osteosarcoma. PLOS ONE, 14(4), e0215312. https://doi.org/10.1371/journal.pone.0215312

Lee, H. C., Fadaili, Y., & Stern, C. D. (2025). Development and functions of the area opaca of the chick embryo. Developmental Biology, 519, 13–20. https://doi.org/10.1016/j.ydbio.2024.12.002

Lin, X., Jin, Z., Li, S., Zheng, M., Xing, Y., Liu, X., Lv, M., Zhao, M., Geng, T., Gong, D., Zhao, D., & Liu, L. (2023). Preliminary study on expression and function of the chicken w chromosome gene mier3 in embryonic gonads. International Journal of Molecular Sciences, 24(10), 8891. https://doi.org/10.3390/ijms24108891

Lindgren, I., Zoer, B., Altimiras, J., & Villamor, E. (2010). Reactivity of chicken chorioallantoic arteries, avian homologue of human fetoplacental arteries. *Journal of Physiology and Pharmacology: An Official Journal of the Polish Physiological Society*, *61*(5), 619–628.

Lokman, N. A., Elder, A. Sf., Ween, M. P., Pyragius, C. E., Hoffmann, P., Oehler, M. K., & Ricciardelli, C. (2013). Annexin A2 is regulated by ovarian cancer-peritoneal cell interactions and promotes metastasis. Oncotarget, 4(8), 1199–1211. https://doi.org/10.18632/oncotarget.1122

Mahajan, D., Kancharla, S., Kolli, P., Sharma, A. K., Singh, S., Kumar, S., Mohanty, A. K., & Jena, M. K. (2021). Role of fibulins in embryonic stage development and their involvement in various diseases. Biomolecules, 11(5), 685. https://doi.org/10.3390/biom11050685

Makanya, A. N., Dimova, I., Koller, T., Styp-Rekowska, B., & Djonov, V. (2016). Dynamics of the developing chick chorioallantoic membrane assessed by stereology, allometry,

immunohistochemistry and molecular analysis. *PLOS ONE*, *11*(4), e0152821. https://doi.org/10.1371/journal.pone.0152821

Mine, Y., Guyonnet, V., Hatta, H., Nau, F., & Qiu, N. (2023). *Handbook of egg science and technology* (1st ed.). CRC Press. https://doi.org/10.1201/9781003254430

Missirlis, E., Karakiulakis, G., & Maragoudakis, M. E. (1990). Angiogenesis is associated with collagenous protein synthesis and degradation in the chick chorioallantoic membrane. Tissue & Cell, 22(4), 419–426. https://doi.org/10.1016/0040-8166(90)90071-g

Miura, K., Koyanagi-Aoi, M., Maniwa, Y., & Aoi, T. (2023). Chorioallantoic membrane assay revealed the role of TIPARP (2,3,7,8-tetrachlorodibenzo-p-dioxin-inducible poly (ADP-ribose) polymerase) in lung adenocarcinoma-induced angiogenesis. Cancer Cell International, 23(1), 34. https://doi.org/10.1186/s12935-023-02870-5

Mojiri, A., Stoletov, K., Lorenzana Carrillo, M. A., Willetts, L., Jain, S., Godbout, R., Jurasz, P., Sergi, C. M., Eisenstat, D. D., Lewis, J. D., & Jahroudi, N. (2016). Functional assessment of von Willebrand factor expression by cancer cells of non-endothelial origin. Oncotarget, 8(8), 13015–13029. https://doi.org/10.18632/oncotarget.14273

Moreau, T., Gautron, J., Hincke, M. T., Monget, P., Réhault-Godbert, S., & Guyot, N. (2022). Antimicrobial proteins and peptides in avian eggshell: Structural diversity and potential roles in biomineralization. Frontiers in Immunology, 13, 946428. https://doi.org/10.3389/fimmu.2022.946428

Moreno-Jiménez, I., Hulsart-Billstrom, G., Lanham, S. A., Janeczek, A. A., Kontouli, N., Kanczler, J. M., Evans, N. D., & Oreffo, R. O. (2016). The chorioallantoic membrane (Cam) assay for the study of human bone regeneration: A refinement animal model for tissue engineering. *Scientific Reports*, *6*(1), 32168. https://doi.org/10.1038/srep32168

Narbaitz, R., Kacew, S., & Sitwell, L. (1981). Carbonic anhydrase activity in the chick embryo chorioallantois: Regional distribution and vitamin D regulation*. Development, 65(1), 127–137. https://doi.org/10.1242/dev.65.1.127

Naushad Khan, et al. *Poultry Farming Industry Contribution in the World Economy*. 2021. *DOI.org (Datacite)*, https://doi.org/10.13140/RG.2.2.22054.86081.

Nowak-Sliwinska, P., Segura, T., & Iruela-Arispe, M. L. (2014). The chicken chorioallantoic membrane model in biology, medicine and bioengineering. Angiogenesis, 17(4), 779–804. https://doi.org/10.1007/s10456-014-9440-7

Nowak-Sliwinska, P., van Beijnum, J. R., van Berkel, M., van den Bergh, H., & Griffioen, A. W. (2010). Vascular regrowth following photodynamic therapy in the chicken embryo chorioallantoic membrane. Angiogenesis, 13(4), 281–292. https://doi.org/10.1007/s10456-010-9185-x

Oudshoorn, B. (2023, November 28). Ella, but from an egg's perspective. *In Ovo*. https://inovo.nl/ella-but-from-an-eggs-perspective/

Pin, A.-L., Houle, F., Fournier, P., Guillonneau, M., Paquet, É. R., Simard, M. J., Royal, I., & Huot, J. (2012). Annexin-1-mediated endothelial cell migration and angiogenesis are regulated by vascular endothelial growth factor (Vegf)-induced inhibition of mir-196a expression. Journal of Biological Chemistry, 287(36), 30541–30551. https://doi.org/10.1074/jbc.M112.393561

Réhault-Godbert, S., Labas, V., Helloin, E., Hervé-Grépinet, V., Slugocki, C., Berges, M., Bourin, M.C., Brionne, A., Poirier, J.-C., Gautron, J., Coste, F., & Nys, Y. (2013). Ovalbumin-related protein x is a heparin-binding ov-serpin exhibiting antimicrobial activities. The

Journal of Biological Chemistry, 288(24), 17285–17295. https://doi.org/10.1074/jbc.M113.469759

Ribatti, D. (2016). The chick embryo chorioallantoic membrane (Cam). A multifaceted experimental model. Mechanisms of Development, 141, 70–77. https://doi.org/10.1016/j.mod.2016.05.003

Ribatti, D. (2017). The chick embryo chorioallantoic membrane (Cam) assay. *Reproductive Toxicology*, *70*, 97–101. https://doi.org/10.1016/j.reprotox.2016.11.004

Ribatti, D. (2025). Lymphatics in the chick embryo chorioallantoic membrane. *Microvascular Research*, *160*, 104806. https://doi.org/10.1016/j.mvr.2025.104806

Ribatti, D., Tamma, R., & Annese, T. (2021). Chorioallantoic membrane vascularization. A meta-analysis. Experimental Cell Research, 405(2), 112716. https://doi.org/10.1016/j.yexcr.2021.112716

Rieder, E., Gay, C. V., & Schraer, H. (1980). Autoradiographic localization of carbonic anhydrase in the developing chorioallantoic membrane. Anatomy and Embryology, 159(1), 17–31. https://doi.org/10.1007/BF00299252

Riley, H. J., & Bradshaw, A. D. (2020). The influence of the extracellular matrix in inflammation: Findings from the sparc-null mouse. The Anatomical Record, 303(6), 1624–1629. https://doi.org/10.1002/ar.24133

Rivera, L. B., Bradshaw, A. D., & Brekken, R. A. (2011). The regulatory function of SPARC in vascular biology. Cellular and Molecular Life Sciences, 68(19), 3165–3173. https://doi.org/10.1007/s00018-011-0781-8

Sarnella, A., Ferrara, Y., Terlizzi, C., Albanese, S., Monti, S., Licenziato, L., & Mancini, M. (2024). The chicken embryo: An old but promising model for in vivo preclinical research. *Biomedicines*, *12*(12), 2835. https://doi.org/10.3390/biomedicines12122835

Saxena, I., & Tayyab, S. (1997). Protein proteinase inhibitors from avian egg whites. Cellular and Molecular Life Sciences CMLS, 53(1), 13–23. https://doi.org/10.1007/PL00000575

Senger, D. R., & Davis, G. E. (2011). Angiogenesis. Cold Spring Harbor Perspectives in Biology, 3(8), a005090–a005090. https://doi.org/10.1101/cshperspect.a005090

Singh, S., Brocker, C., Koppaka, V., Ying, C., Jackson, B., Matsumoto, A., Thompson, D. C., & Vasiliou, V. (2013). Aldehyde dehydrogenases in cellular responses to oxidative/electrophilic stress. Free Radical Biology & Medicine, 56, 89–101. https://doi.org/10.1016/j.freeradbiomed.2012.11.010

Soulet, F., Kilarski, W. W., Roux-Dalvai, F., Herbert, J. M. J., Sacewicz, I., Mouton-Barbosa, E., Bicknell, R., Lalor, P., Monsarrat, B., & Bikfalvi, A. (2013). Mapping the extracellular and membrane proteome associated with the vasculature and the stroma in the embryo. Molecular & Cellular Proteomics : MCP, 12(8), 2293–2312. https://doi.org/10.1074/mcp.M112.024075

Süß, S. C., Werner, J., Saller, A. M., Weiss, L., Reiser, J., Ondracek, J. M., Zablotski, Y., Kollmansperger, S., Anders, M., Potschka, H., Schusser, B., Fenzl, T., & Baumgartner, C. (2023). Nociception in chicken embryos, part iii: Analysis of movements before and after application of a noxious stimulus. Animals, 13(18), 2859. https://doi.org/10.3390/ani13182859

Tagirov, M., & Golovan, S. (2015). Sexual dimorphism in the early embryogenesis of the chicken (gallus gallus domesticus): Sexual dimorphism in early embryogenesis. Molecular Reproduction and Development, 82(5), 332–343. https://doi.org/10.1002/mrd.22476

Tetlow, N., & Board, P. G. (2004). Functional polymorphism of human glutathione transferase A2: Pharmacogenetics, 14(2), 111–116. https://doi.org/10.1097/00008571-200402000-00005

Tong, Q., Romanini, C. E., Exadaktylos, V., Bahr, C., Berckmans, D., Bergoug, H., Eterradossi, N., Roulston, N., Verhelst, R., McGonnell, I. M., & Demmers, T. (2013). Embryonic development and the physiological factors that coordinate hatching in domestic chickens. *Poultry Science*, *92*(3), 620–628. https://doi.org/10.3382/ps.2012-02509

Tsopanoglou, N. E., Pipili-Synetos, E., & Maragoudakis, M. E. (1993). Thrombin promotes angiogenesis by a mechanism independent of fibrin formation. The American Journal of Physiology, 264(5 Pt 1), C1302-1307. https://doi.org/10.1152/ajpcell.1993.264.5.C1302

Tu, Z., Lin, Y.-N., & Lin, C.-H. (2013). Development of fucosyltransferase and fucosidase inhibitors. Chemical Society Reviews, 42(10), 4459–4475. https://doi.org/10.1039/C3CS60056D

Tuan, R. S. (1984). Carbonic anhydrase and calcium transport function of the chick embryonic chorioallantoic membrane. Annals of the New York Academy of Sciences, 429(1), 459–472. https://doi.org/10.1111/j.1749-6632.1984.tb12372.x

Tuan, R. S., & Zrike, J. (1978). Functional involvement of carbonic anhydrase in calcium transport of the chick chorioallantoic membrane. The Biochemical Journal, 176(1), 67–74. https://doi.org/10.1042/bj1760067

Tuan, R. S., Carson, M. J., Jozefiak, J. A., Knowles, K. A., & Shotwell, B. A. (1986). Calcium-transport function of the chick embryonic chorioallantoic membrane: I. in vivo and in vitro characterization. Journal of Cell Science, 82(1), 73–84. https://doi.org/10.1242/jcs.82.1.73

Wang, S., He, X., Wu, Q., Jiang, L., Chen, L., Yu, Y., Zhang, P., Huang, X., Wang, J., Ju, Z., Min, J., & Wang, F. (2020). Transferrin receptor 1-mediated iron uptake plays an essential role in hematopoiesis. Haematologica, 105(8), 2071–2082. https://doi.org/10.3324/haematol.2019.224899

Wang, Y., Branicky, R., Noë, A., & Hekimi, S. (2018). Superoxide dismutases: Dual roles in controlling ROS damage and regulating ROS signaling. The Journal of Cell Biology, 217(6), 1915–1928. https://doi.org/10.1083/jcb.201708007

Wang, Y., Wang, M., Shan, A., & Feng, X. (2020). Avian host defense cathelicidins: Structure, expression, biological functions, and potential therapeutic applications. Poultry Science, 99(12), 6434–6445. https://doi.org/10.1016/j.psj.2020.09.030

Wasik, A., Ratajczak-Wielgomas, K., Badzinski, A., Dziegiel, P., & Podhorska-Okolow, M. (2022). The role of periostin in angiogenesis and lymphangiogenesis in tumors. Cancers, 14(17), 4225. https://doi.org/10.3390/cancers14174225

Yáñez, M., Gil-Longo, J., & Campos-Toimil, M. (2012). Calcium binding proteins. In Md. S. Islam (Ed.), Calcium Signaling (pp. 461–482). Springer Netherlands. https://doi.org/10.1007/978-94-007-2888-2_19

Yang, H., Lee, B. R., Lee, S., Ock, S. A., Oh, K. B., Jo, Y. J., Lee, P., Lee, H., Han, J. Y., & Byun, S. J. (2024). Improved surrogate eggshell incubation system for assisted reproductive technologies such as cloning, genome modification, and de-extinction efforts. Scientific Reports, 14(1), 20796. https://doi.org/10.1038/s41598-024-71804-6

Yang, S., Wang, L. L., Shi, Z., Ou, X., Wang, W., Chen, X., & Liu, G. (2018). Transcriptional profiling of liver tissues in chicken embryo at day 16 and 20 using RNA sequencing reveals differential antioxidant enzyme activity. PLoS ONE, 13(2), e0192253. https://doi.org/10.1371/journal.pone.0192253

Yuan, Z.-Y., Cheng, L.-T., Wang, Z.-F., & Wu, Y.-Q. (2021). Desmoplakin and clinical manifestations of desmoplakin cardiomyopathy. Chinese Medical Journal, 134(15), 1771–1779. https://doi.org/10.1097/CM9.0000000000001581

Zhang, Y., Goss, A. M., Cohen, E. D., Kadzik, R., Lepore, J. J., Muthukumaraswamy, K., Yang, J., DeMayo, F. J., Whitsett, J. A., Parmacek, M. S., & Morrisey, E. E. (2008). A Gata6-Wnt pathway required for epithelial stem cell development and airway regeneration. Nature Genetics, 40(7), 862–870. https://doi.org/10.1038/ng.157

Zhang, Y., Zheng, X., Zhang, Y., Zhang, H., Zhang, X., & Zhang, H. (2020). Comparative transcriptomic and proteomic analyses provide insights into functional genes for hypoxic adaptation in embryos of Tibetan chickens. Scientific Reports, 10(1), 11213. https://doi.org/10.1038/s41598-020-68178-w